Mercury Open Water Final Report for Compliance with the Delta Mercury Control Program

Chapter 4.-Yolo Bypass - Mercury and Methylmercury Modeling Studies

Submitted by the Open Water Mercury Modeling Work Team

Aug 31, 2020

The Open Water Mercury Modeling Workgroup

California Department of Water Resources — Division of Environmental Sciences
Carol DiGiorgio
David Bosworth

California Department of Water Resources — Bay Delta Office
Prabhjot Sandhu
Ali Abrishamchi
Jamie Anderson
Hans Kim
Kevin He
En-Ching Hsu
Kijin Nam
Hari Rajbhandari
Min-Yen Yu
Tara Smith
Eli Ateljevich

Reed Harris Environmental Ltd.
Reed Harris
David Hutchinson.
Matt Gove
Cody Beals
Don Beals

U.S. Geological Survey — Upper Midwest Science Center
Randy Hunt

Acknowledgements

We wish to acknowledge the provision of data and ideas from Mark Stephenson and Wes Heim at the Moss Landing Marine Laboratories, Gary Gill of the Pacific Northwest National Laboratory, and Paul Work, David Schoellhamer, Charles Alpers, Mark Marvin-DiPasquale, Lisa Marie Windham-Myers and David Krabbenhoft at the US Geological Survey. Many thanks also to Helen Amos who provided a major contribution to the early stages of the Yolo Bypass analysis.

Contents

List of Figures

List of Tables

List of Acronyms and Abbreviations

CVRWQCB	Central Valley Regional Water Quality Control Board
CCSB	Cache Creek Settling Basin
cfs	Cubic Feet per Second
Delta	Sacramento-San Joaquin Delta
D-MCM	Dynamic Mercury Cycling Model
DOC	Dissolved Organic Carbon
DMCP	Delta Mercury Control Program (DMCP)
DWR	(California) Department of Water Resources
fHg	filtered Hg
fMeHg	filtered MeHg
GIS	Geographic Information System
Hg	Mercury
Hg(II)	Inorganic Hg in oxidized state (+2)
Hg(0)	Elemental Mercury
Inorganic Hg	Sum of Hg(II) and Hg(0)
KLRC	Knights Landing Ridge Cut
MeHg	Methylmercury
PEST ++	Parameter Estimation Software
THg	Total Mercury-sum of all forms of inorganic Hg and MeHg
TSS	Total Suspended Solids
uHg	An unfiltered (aqueous) mercury (sample)
uMeHg	An unfiltered (aqueous) methylmercury (sample)
WY	Water Year(s)

Introduction-Yolo Bypass Mercury and Methylmercury Modeling

The Delta Mercury Control Program (DMCP) requires the (California) Department of Water Resources (DWR) to reduce methylmercury (MeHg) open water sediment flux from areas out of compliance in the Sacramento-San Joaquin Delta (Delta) and the Yolo Bypass (See Chapter 1). Application of a mercury (Hg) mass balance mechanistic model, complemented by field data and laboratory approaches, was approved by the Central Valley Regional Water Quality Control Board (Regional Board) to pursue and evaluate options to reduce MeHg supply from open water sediments via operational changes. Chapter 3 summarized the scientific studies conducted as part of the approved Workplan. The objective of Chapter 4 is to summarize and provide key findings of interest associated with model development and model findings to management and policy makers for the Yolo Bypass, based on the application of the Dynamic Mercury Cycling Model (D-MCM). While D-MCM is a proprietary model (EPRI, 2013) the approach to Hg cycling in D-MCM has been published (Harris and others, 2012, Hudson and others, 1994). In addition to the Technical Appendix, any model input and output information is available on request.

Site Description

The Yolo Bypass

The Yolo Bypass is a 3-mile wide, 40 mile-long, 59,000-acre flood conveyance system that diverts flood waters from the Sacramento River around the City of Sacramento (Figure 4-1). The Yolo Bypass floods in roughly 7 out of 10 years with inundation occurring typically between October and April. When completely flooded, the Yolo Bypass approximately doubles the wetted area of the Delta (Schmitt, 2011) and can carry up to four times the flow of the Sacramento River's main channel during large floods (Suddeth Grimm and Lund, 2016). The project design capacity is 343,000 cfs (DWR, 2010).

The primary source of water to the Yolo Bypass is the 2-mile wide Fremont Weir where water passively flows into the Yolo Bypass when the Sacramento river reaches 32 feet stage height (NAVD88 datum) or approximately 60,000 cfs. Additional tributaries into the Yolo Bypass include the Knight's Landing Ridge Cut (KLRC), the Cache Creek Overflow weir and low flow channel for the Cache Creek Settling Basin (CCSB), Willow Slough and Putah Creek (Figure 4-1). Depending on flood flows, the flood gates of the Sacramento Weir can also be opened. The dominant hydrological feature at the southern end of the Yolo Bypass is Liberty Island, a 5,300-acre parcel of open water and wetland habitat that is tidally influenced except during large floods in the Yolo Bypass. Just north of Liberty Island is the feature referred to as the Stairsteps drainage canals (Figure 4-1).

Figure 4-1. Yolo Bypass Schematic Map

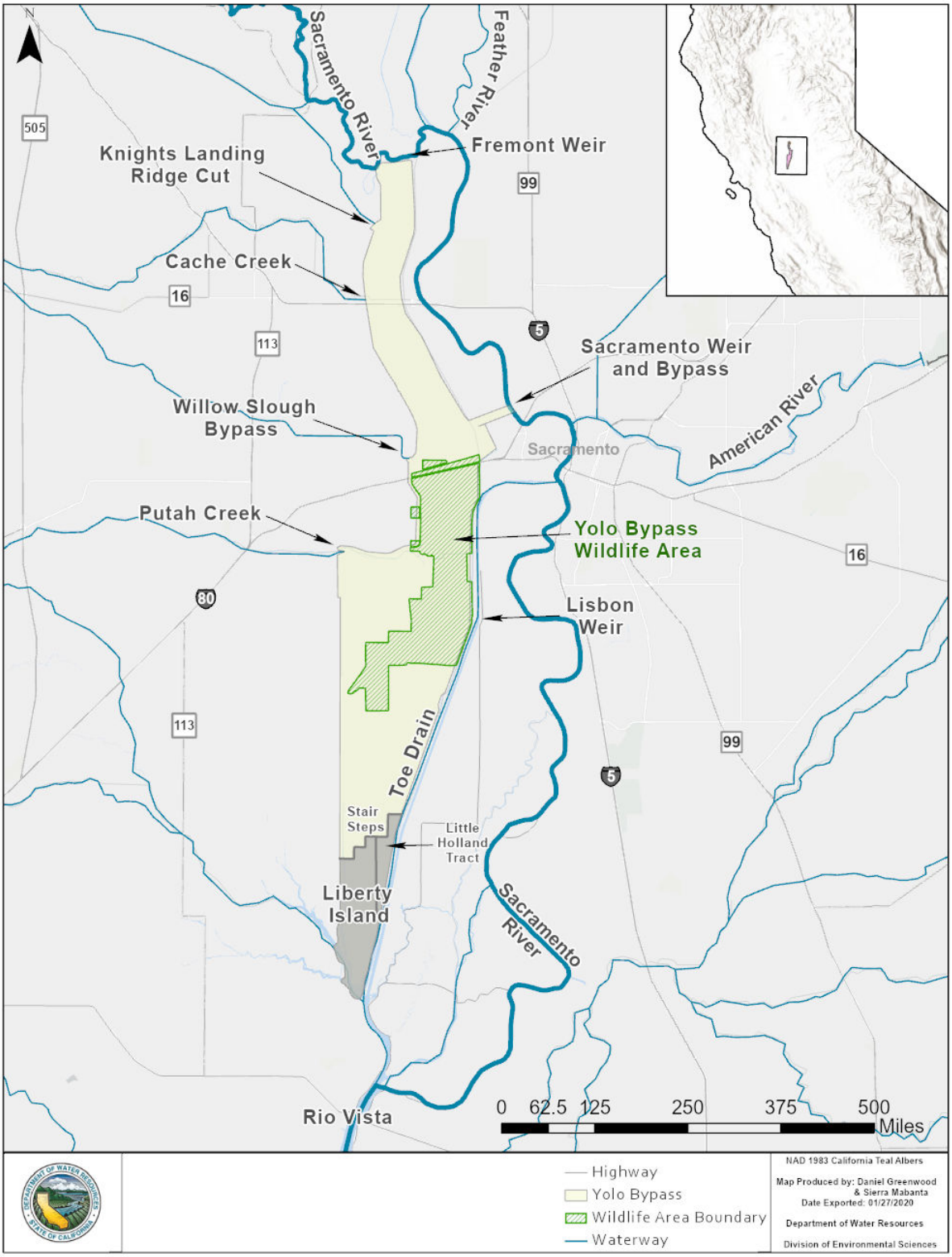

Study Objectives and Approach

Objectives

The primary objectives associated with developing a biogeochemical Hg cycling model to the Yolo Bypass were to:

- Create a model that can simulate concentrations, fluxes, transport and fate of inorganic Hg and MeHg in water and surface sediments in the Yolo Bypass.
- Use the model to evaluate processes governing MeHg supply to the Yolo Bypass.
- Use the model to help evaluate whether there are operational changes or other strategies that can be implemented to reduce ambient MeHg concentrations in Yolo Bypass floodwaters.

Model Integration with other Project Studies

The overall project included studies based on mechanistic modelling, field and laboratory data (Figure 4-2, Table 4-1). The model analysis was designed to primarily use existing models and data. Supplemental additional studies were carried out to provide information needed to better characterize conditions affecting Hg, and specifically MeHg loads, in the Yolo Bypass. Summary results for the studies in Figure 4-2 other than modeling can be found in Chapter 3, as well as detailed information in the Technical Appendices.

Figure 4-2 Yolo Bypass Modeling, Field and Experimental Study Components

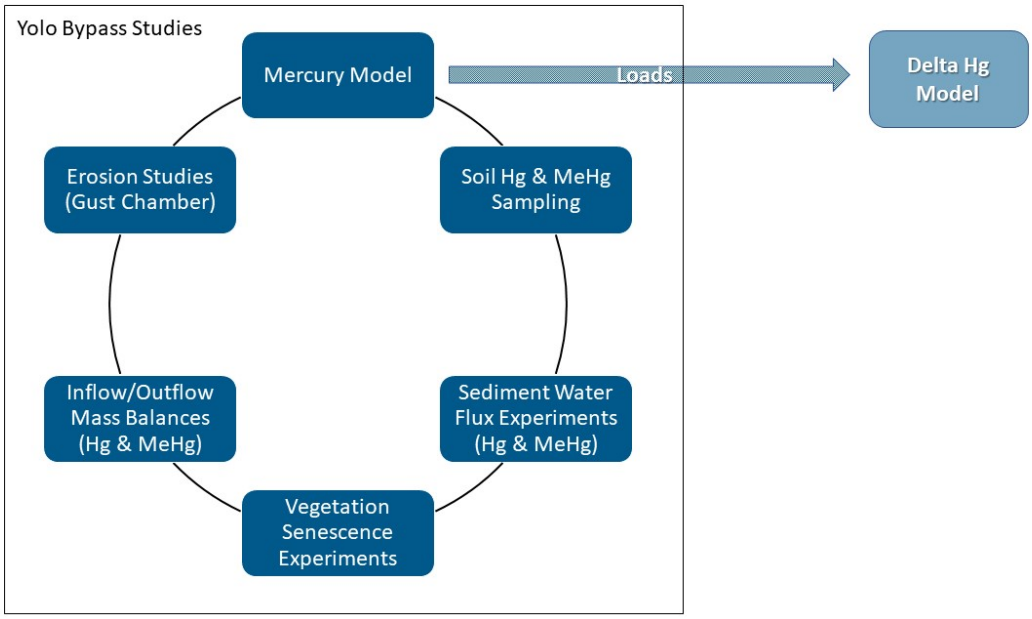

Table 4-1 Studies Carried Out to Support Modelling

Information Source	Information Provided	How was the Information Used?
2017 Yolo Bypass Mass Balance Study	Hg, MeHg, TSS, and other water chemistry concentrations and fluxes at inlet, outlet and intermediate locations in the Yolo Bypass.	Development of boundary tributary fluxes for suspended sediment, Hg and MeHg Used to help calibrate Hg and MeHg partitioning between solids and dissolved phase in model. Comparison with model results for other years, whether the Yolo Bypass is a source or sink for sediments, Hg and MeHg
Sediment-water Flux Study	THg and MeHg concentrations in pore water and sediment solids. Pore-water chemistry (DOC, pH, etc.)	Combined with other data to help calibrate Hg concentrations in surface sediments in model. Used to help calibrate dissolved fluxes of Hg and MeHg from sediments to overlying water in model.
Soil Hg concentration study	Soil concentrations of Hg and MeHg in different land uses and locations in the Yolo Bypass	Contributed to data used to estimate Hg and MeHg concentrations in surface soils in the Yolo Bypass Used to help calibrate surface sediment concentrations of Hg and MeHg in model. Used to help calibrate model resuspension fluxes of Hg and MeHg from sediments to water in model.
Gust Chamber Erosion Study	Sediment resuspension rates for different flow velocities and shear stresses, in different land uses in the Yolo Bypass	Assisted to estimate sediment resuspension rates in the Yolo Bypass as a function of flow.
Vegetation Senescence Studies	Effects of vegetation on MeHg production.	Contributed to model calibration of effects of vegetation Provided information to compare with results of model simulations of effects of removing vegetation

Model Selection

At the time of Workplan approval, no single model existed to adequately simulate hydrology, sediment transport and Hg cycling in the Delta and/or Yolo Bypass. For the Yolo Bypass, two existing models were used in combination, one simulated hydrology and the other simulated sediment transport and Hg in water and sediments. Both models were capable of 2D simulations needed for the Yolo Bypass. Hg simulations explicitly followed MeHg and two forms of inorganic Hg (Hg(II) and Hg(0)). The Yolo Bypass was simulated first, and results were then passed to the Delta Model (see Chapter 5). The modeling domain for the two models is shown in Figure 4-3. The model analysis did not simulate MeHg in the food web, as the key end point was MeHg loads from sediments to open waters.

Figure 4-3. Modeling Domains for Yolo Bypass D-MCM and the DSM2-Hg Models

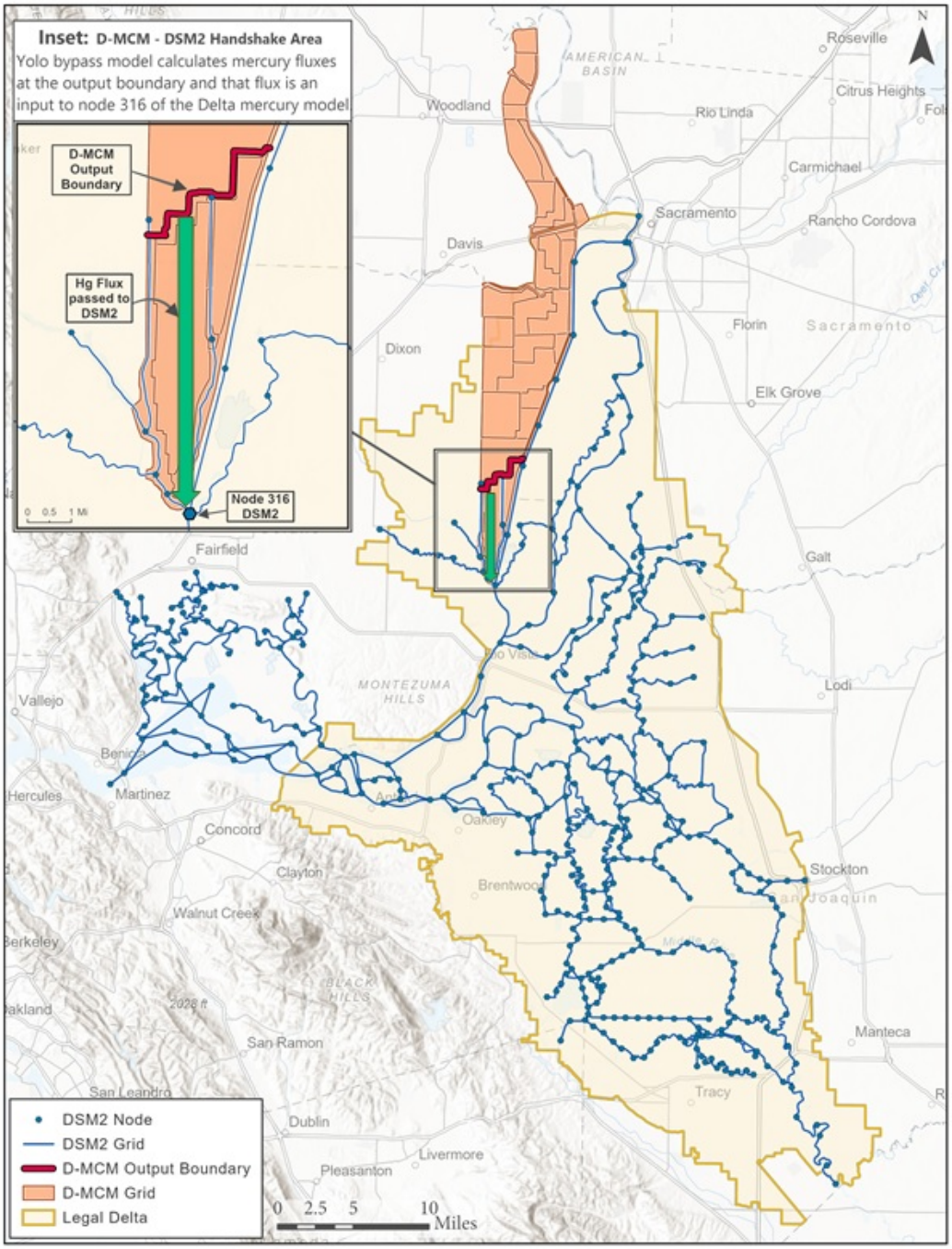

From the Hg perspective, the Yolo Bypass is especially challenging to simulate because conditions affecting Hg cycling, including MeHg supply, are highly variable and change quickly. Most of the Yolo Bypass is intermittently wet and dry, a situation known to affect MeHg production, but difficult to quantify. There have also been many human activities in the Yolo Bypass beyond flood control, including rice agriculture, and management of seasonal wetland and pasture habitats. These land uses affect site conditions that influence MeHg supply, for example hydrology and the supply of organic matter.

The Dynamic Mercury Cycling Model (v4.0, EPRI, 2013) was chosen to model Hg and MeHg in the water column and sediment bed in the Yolo Bypass. The D-MCM is a Windows-based simulation model for personal computers. A summary of the approach used in D-MCM to represent Hg cycling in aquatic systems is presented in a later section. Previous versions of D-MCM have been used in large multidisciplinary research projects in the Gulf of Mexico (Harris and others, 2012a), Florida Everglades (Harris and others, 2003a), METAALICUS (Harris and others, 2007), and Wisconsin Lakes (Hudson and others, 1994). It has also been used in pilot TMDL studies in Florida (Atkeson and others, 2003) and Wisconsin (Harris and others, 2003b) and a model analysis of the effects of climate change on Hg cycling and bioaccumulation in the Great Lakes Basin, funded by the US EPA (Harris and others, 2015, 2012b).

Major Components of Model Analysis – Yolo Bypass

Application of D-MCM to the Yolo Bypass included the following steps:

1. Development of model grid
2. Estimates of hydrology
3. Estimates of suspended sediment loads (other than vegetation)
4. Incorporation of vegetation
5. Calibration of the model to available data for suspended sediments and Hg
6. Sensitivity/uncertainty analysis, and
7. Simulations of sensitivity runs agreed to with Regional Board

Model Grid Development

D-MCM was set up for the Yolo Bypass using a coarse spatial resolution with 47 cells, each assumed to have uniform characteristics internally. D-MCM is not a high spatial resolution model, and a finer spatial scale analysis would also not have been adequately supported with the level of data available and the uncertainties regarding some aspects of Hg cycling within the Yolo Bypass (e.g. effects of vegetation and wetting/drying). The model grid reflected 5 GIS layers that considered the following features:

- Land use
- Hg and MeHg concentrations in sediments
- Agricultural disking (the model calibration did not distinguish disked/undisked areas)
- Hydrology - Fraction of time wet
- Hydrology - wet/dry cycling frequency

Multiple land uses within the Yolo Bypass were grouped as follows to develop the model grid: pasture, fallow, white rice, wild rice, seasonal wetlands, tidal marshes, mixed other, and water conveyance channels. Individual parcels of land in the Yolo Bypass used for various purposes were too small to be represented individually in the model analysis. Therefore, model cells were set up, to the extent possible, to include a single dominant land use within each cell, while maintaining the same overall fractions of land used for different purposes in the Yolo Bypass. Information on land used for crops was drawn primarily from a 2005-2009 survey conducted by Howitt and others (2013). Land use data in the Yolo Wildlife Area were obtained from the Yolo Wildlife Area manager. In addition, wetland GIS data developed by Duck's Unlimited for the Delta Methylmercury TMDL TMDL Nonpoint Source

Workgroup (NPS Workgroup, 2012) and the National Wetlands Inventory were also examined (U.S. Fish and Wildlife Service, 2020).

Surface sediment concentrations of Hg and MeHg vary within the Yolo Bypass. Characterization of the spatial variability of surface sediment Hg and MeHg concentrations was carried out using data from 1999-2016 (see additional discussion later in Chapter).

Frequency of land wetting and frequency of wet/dry cycling have the potential to stimulate Hg methylation. These factors were characterized using outputs from previous hydrodynamic simulations carried out for 1997-2012 using a model called TUFLOW (additional information is provided later in the Chapter). Frequency of wetting was calculated as the percentage of wet days in TUFLOW simulations in a given TUFLOW cell. Wet/dry cycling was defined as the average number of wet/dry cycles per year in TUFLOW simulations. GIS layers were created for each factor, and both displayed a slight east to west gradient across the Yolo Bypass.

The final model grid is shown in Figure 4-4. It features 17 permanently wet cells (classified as water) and 30 land (seasonally wet) cells classified under different land use types. Additional details on the development of the model grid are available in the 2015 Progress Report (DWR, 2015).

Outputs from the Yolo Bypass model were passed to the Delta model at the stairsteps. This location was chosen rather than the bottom of Liberty Island because flows at the stairsteps are primarily in one direction (downstream). Conditions below the stairsteps do not have a large effect on Hg above the stairsteps.

Figure 4-4 Model Grid Used for the Yolo Bypass Dynamic Mercury Cycling Model

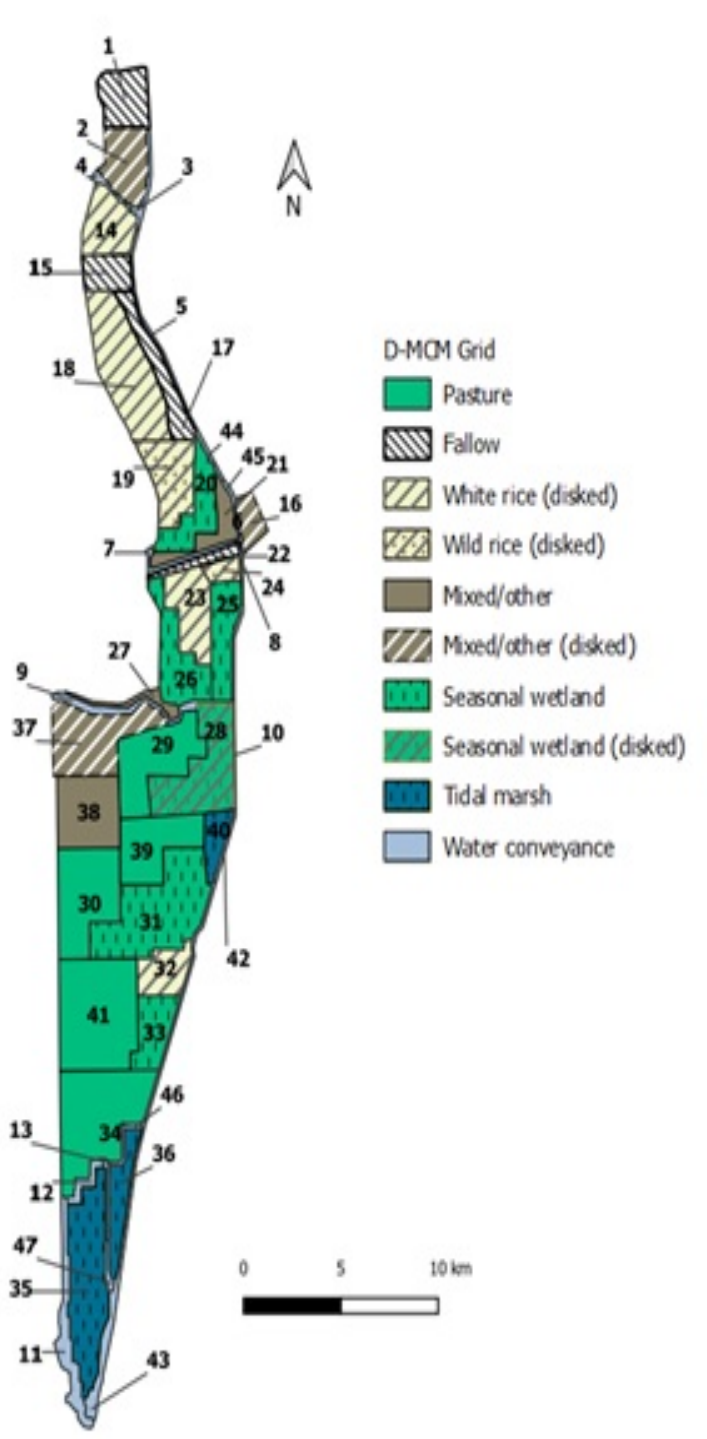

Cell #	Land use
1	Fallow
2	Mixed/other
3	Water
4	Water
5	Water
6	Water
7	Water
8	Water
9	Water
10	Water
11	Water
12	Water
13	Water
14	White rice
15	Fallow
16	Mixed/other
17	Fallow
18	White rice
19	Wild rice
20	Wetland
21	Mixed/other
22	Fallow
23	White rice
24	Wild rice
25	Wetland
26	Wetland
27	Mixed/other
28	Wetland
29	Pasture
30	Pasture
31	Wetland
32	White rice
33	Wetland
34	Pasture
35	Tidal marsh
36	Tidal marsh
37	Mixed/other
38	Mixed/other
39	Pasture
40	Tidal marsh
41	Pasture
42	Water
43	Water
44	Water
45	Water
46	Water
47	Water

Model Approach

Approach to Hydrology

Hydrology for D-MCM simulations must be estimated externally to the model and then provided as input information. For this study, hydrology was available from a hydrodynamic model called TUFLOW (www.tuflow.com), previously developed for DWR as part of an EIS/EIR for the Yolo Bypass Salmonid Habitat Restoration and Fish Passage Project (DOI/DWR, 2019). TUFLOW outputs were available for Water Years (WY) 1997-2012 (October 1996 - May 2012). Because this was the period that realistic hydrology could be represented in Yolo Bypass simulations, this was also the period that D-MCM was applied to simulate Hg. As shown in Table 4-2 this time period captured a wide range of flow conditions, including some of the wettest years on record with sustained flooding in the Yolo Bypass, and drought years when little or no overtopping of the Fremont weir occurred.

Table 4-2 Index of Sacramento Valley Water Year Classification.

Water Year	Index
1997	W
1998	W
1999	W
2000	AN
2001	D
2002	D
2003	AN
2004	BN
2005	AN
2006	W
2007	D
2008	C
2009	D
2010	BN
2011	W
2012	BN

Water Year classifications from wettest to driest are: W=Wet, AN=Above Normal, BN=Below Normal, D=Dry, C=Critical (CDEC 2020).

TUFLOW simulations used a grid with much higher spatial resolution (approximately 25’ x 25’) than the D-MCM Hg analysis. TUFLOW outputs were aggregated spatially to match the Hg model grid consisting of 47 cells. TUFLOW outputs were also aggregated in time from hourly to daily average estimates.

Hydrology in the Yolo Bypass is complex, with a high degree of human intervention:

a. Flood control: TUFLOW simulations considered natural flows and the management of water for flood control during the wet season from October through May each year but did not simulate summer flows and did not consider other water uses in the Yolo Bypass.

b. Agriculture and wetland management: Rice cultivation occurs in the Yolo Bypass, as well as management of wetland areas where water is added seasonally to enhance waterfowl habitat. Both

of these uses involve water additions and removals. Estimates of water usage for these purposes were calculated in a coarse manner (information available upon request)

To allow a single simulation from October 1996-May 2012, rather than simulate 16 wet seasons separately, summer flows from June-September were generated each year to hydrologically link TUFLOW results for different wet seasons. This was done by calculating summer flows for each model cell that would transition from the water volume at the end of a TUFLOW simulation in May to match the volume of water in October, used to start the next wet season simulation with TUFLOW.

Approach to Represent Suspended and Bed Sediments

D-MCM was set up for the Yolo Bypass with four particle types:

a. Organic matter other than vegetation
b. Vegetation solids.
c. Fine inorganics (e.g. silt and clay)
d. Coarse inorganics (e.g. sand)

Each particle type had unique properties in terms of particle densities, settling velocities, resuspension rates, and Hg partitioning (ratio of solids:dissolved concentrations).

Tributary loads for suspended sediments were estimated using empirical approaches that varied among tributaries. For example, Fremont Weir is an important source of suspended sediments to the Yolo Bypass. Measurements of suspended sediment at Fremont Weir were limited (n=13 in 2006, n=9 in 2016/2017). Daily suspended sediment estimates were available however for the simulation period at Freeport, approximately 36 river miles downstream in the Sacramento River (Sacramento River Forum, 2020). A relationship between suspended sediment concentrations between Fremont Weir and Freeport was developed to estimate daily suspended sediment concentrations at Fremont Weir (see comparison of observed and estimated SSC at Fremont Weir in Figure 4-5). For other tributary inflows to the Yolo Bypass, daily flow estimates were available (from TUFLOW), but daily measurements of other constituents, e.g. suspended sediments, were not. Regressions were developed between suspended sediments and flow for these inflows using limited tributary-specific observations. Daily flow estimates for tributaries from the TUFLOW model were then used to estimate daily suspended sediment concentrations in these inflows to the Yolo Bypass.

Figure 4-5 Regression-Estimated and Field-Measured Concentrations of Suspended Sediments at Fremont Weir in 2006 and 2017

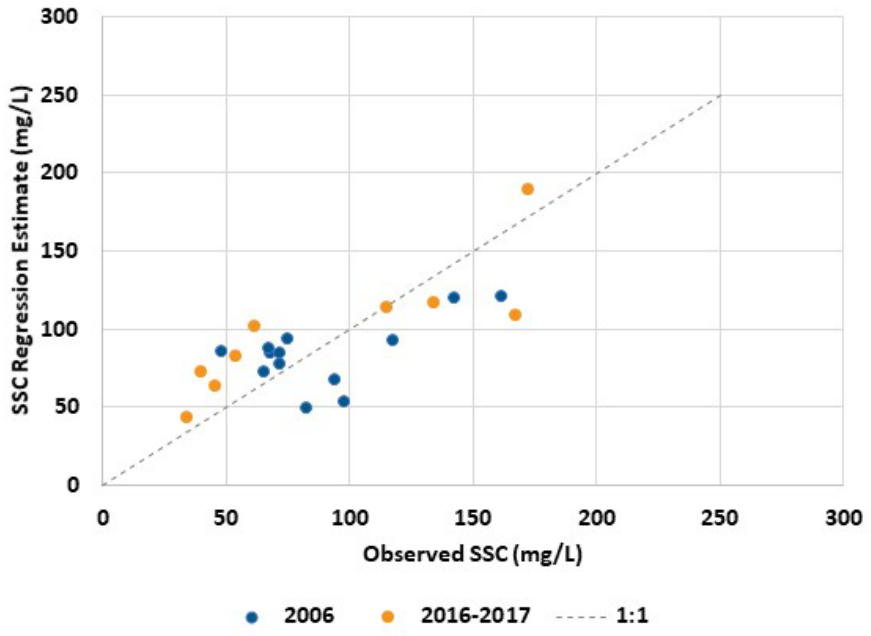

Figure Note: 2006 observations from Foe and others, 2008. 2017 observations from DWR Mass Balance Study.

Once loaded into Yolo Bypass waters, suspended sediments could settle to the sediment bed or remain in suspension. Resuspension of sediments from the sediment bed to overlying water was also included. TUFLOW velocity estimates were used to estimate shear stress and sediment resuspension in the Yolo Bypass at high resolution. These resuspension estimates were summed within each of the 47 Hg model cells and used as inputs to Hg simulations. Terrain-specific erosion experiments were carried out using a Gust chamber to support the model analysis (Technical Appendix D). In the sediment bed, the active surface layer was assigned a thickness of 2 cm and a mass balance was maintained for sediment mass. The difference between inputs (settling) and losses (resuspension and decomposition) determined if there was net accumulation or erosion of the surface sediment layer.

Vegetation also supplied solids to the system during die-off periods each year. Approximately 3/4 of the surface area of the Yolo Bypass upstream of the stairsteps was assigned as pasture, white rice, wild rice or seasonal wetland terrain. When compared to the overall external supply of sediments to the Yolo Bypass, vegetation solids loads were secondary (17%). In terms of the supply of organic matter however, vegetation supplied more than half (63%) and was an important source of carbon supporting wet season MeHg production in simulations.

As shown in Figure 4-6, different seasonal patterns for growth and die-off, and peak biomasses were developed for pasture, wetlands, white rice and wild rice vegetation (Figure 4-6).

Vegetation solids were quickly delivered through the water column to sediments following senescence and were instantly mixed into the surface sediment layer with other sediments. In reality, vegetation solids may remain as a separate compartment from surface sediments, but the current construct of D-MCM did not allow this configuration. Vegetation was assumed to decompose within the sediment bed more easily than other sediments. Overall, the timing, magnitude and fate of vegetation in D-MCM simulations of the Yolo Bypass was viewed as a preliminary treatment that could be refined if future modeling is carried out.

Figure 4-6 Model Inputs for Vegetation Biomass

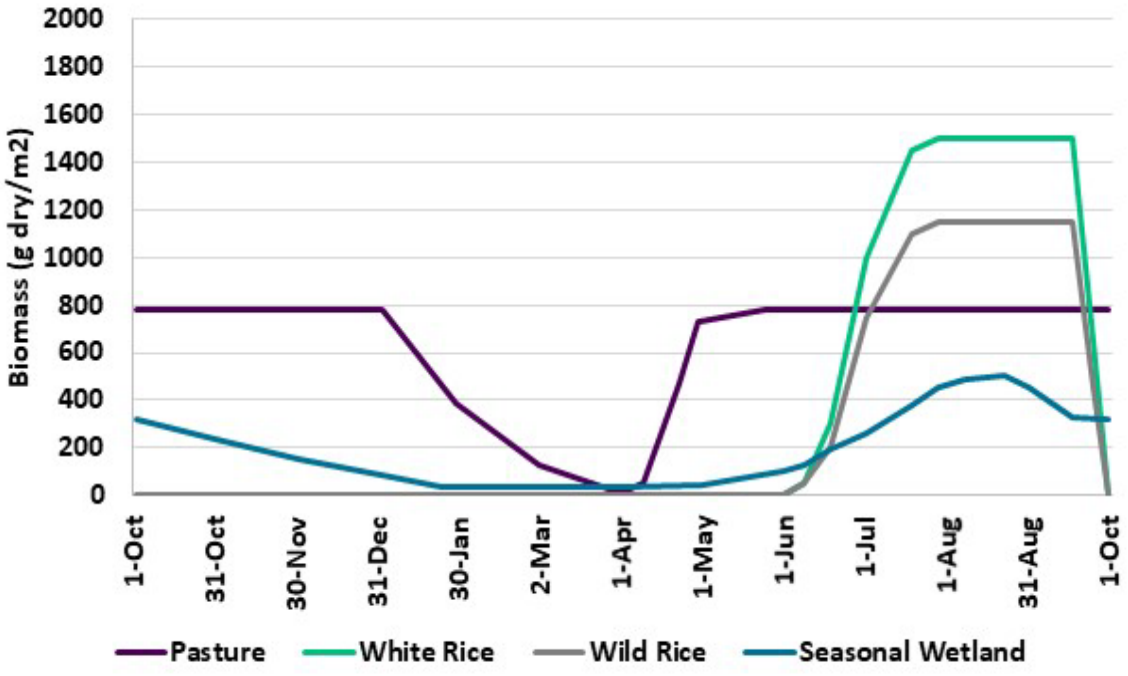

Figure Note: Seasonality of growth and die off was based on Stephenson (2019). Peak biomass values: pasture from Stephenson (2020), white rice and wild rice based on Wyndham-Myers and others (2014), seasonal wetland from Stephenson (2017).

Approach to Represent Hg Cycling

Hg cycling was simulated using the D-MCM model. D-MCM is a time dependent, mechanistic mass balance model for Hg cycling and bioaccumulation, modeling the cycling and fate of three major forms of Hg (MeHg, inorganic Hg (II), and elemental Hg) in aquatic systems. Model compartments include one or more layers in the water column and sediments and can include a food web (not done in this analysis). Key Hg processes in D-MCM are shown in Figure 4-7. D-MCM also includes vegetation, which is important in the Yolo Bypass, where land types include seasonal wetlands, rice agriculture and intermittently flooded pasture lands. Although the effects of vegetation on Hg cycling, and MeHg production in particular, could only be simulated coarsely in D-MCM, this first attempt still provided. insights into the role of vegetation on MeHg supply. The model is capable of simulating systems using a

1, 2 or 3D scheme. For the Yolo Bypass, the D-MCM was set up in a 2D configuration, where conditions varied in the direction of flow and horizontally perpendicular to flow but were well mixed vertically.

Figure 4-7 Schematic Representation of Processes Modeled by The Dynamic Mercury Cycling Model (Vegetation not Shown)

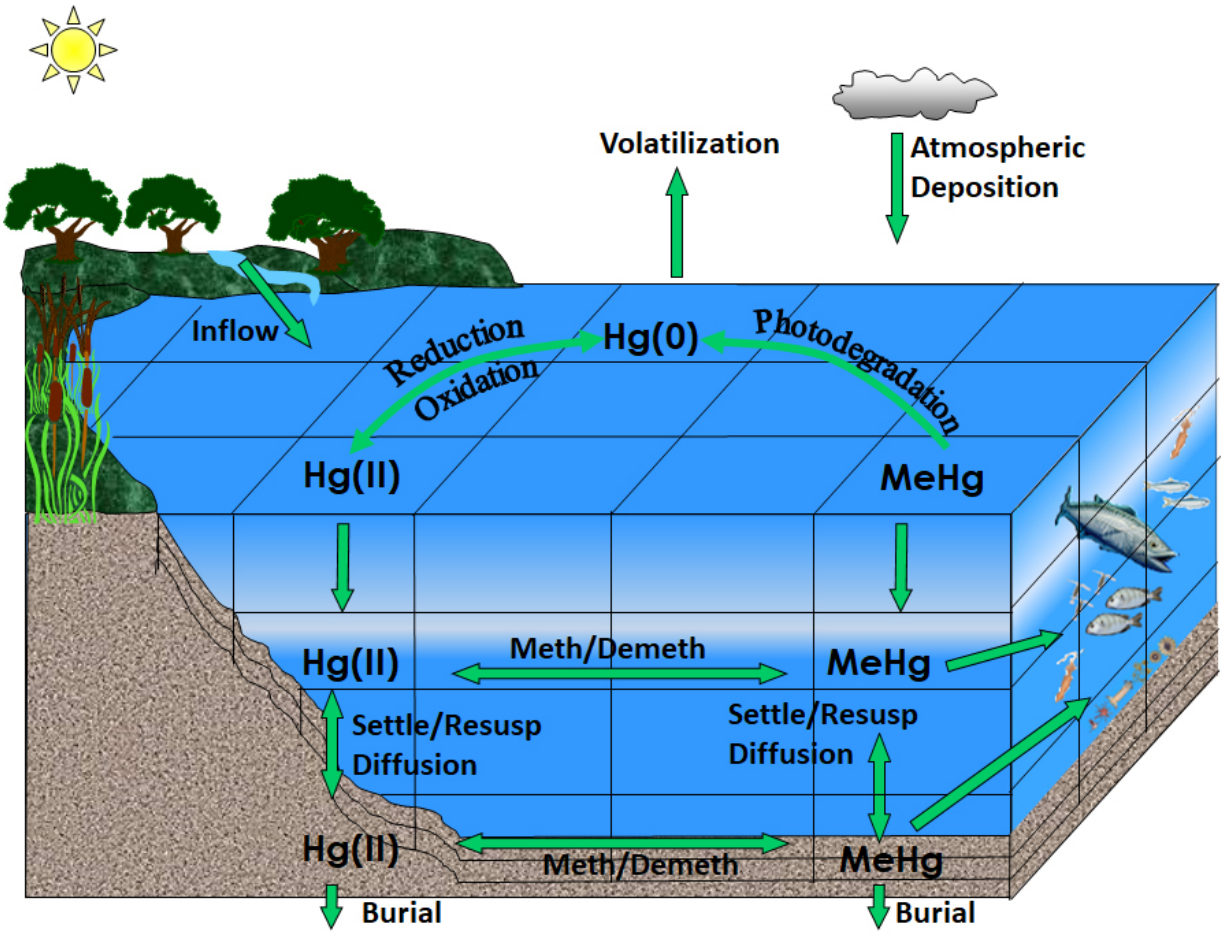

Atmospheric wet deposition of inorganic Hg was estimated using data from the nearest Mercury Deposition Network (MDN) site, CA72, near San Jose. The site was operated from January 11, 2000 through December 27, 2006. Weekly data were used to estimate overall monthly averages for the entire period of record, for use in the DSM2-Hg analysis. Dry Hg deposition was assigned a constant value of 19 ug/m2/yr, the mean value reported by Tsai and Hoenecke (2001) for the San Francisco Bay Estuary from August 1999 through November 2000.

Tributary loads of inorganic uHg and uMeHg were based on empirical relationships between concentrations and flow or TSS (which was subsequently estimated on the basis of flow). This was done using tributary-specific data to the extent possible. For example, comparisons of regression estimates and field-based estimates of uHg and uMeHg loads to the Yolo Bypass for Cache Creek Settling Basin are shown in Figure 4-8 and Figure 4-9.

Figure 4-8 Regression Model versus Field Estimates of uHg Loads to the Yolo Bypass from the Cache Creek Settling Basin

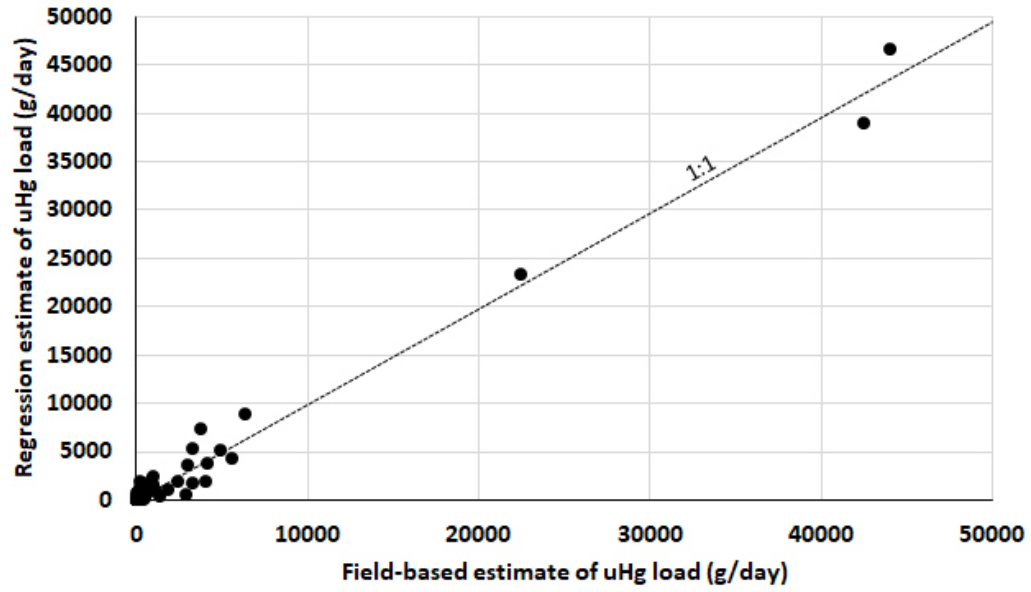

*uHg concentrations were based on daily average flow estimates from TUFLOW model: [$uHg_{(ng/L)}$] = 0.0193 * $Flow_{(cfs)}$ +10 if Flow < 10,600 cfs, [$uHg_{(ng/L)}$] = 0.0966 * $Flow_{(cfs)}$ – 800.36 if Flow> 10,600 cfs,. Data from USGS (2019)*

Figure 4-9 Regression Model Estimates of MeHg Loads to the Yolo Bypass Versus Field-Based Estimates for the Cache Creek Settling Basin

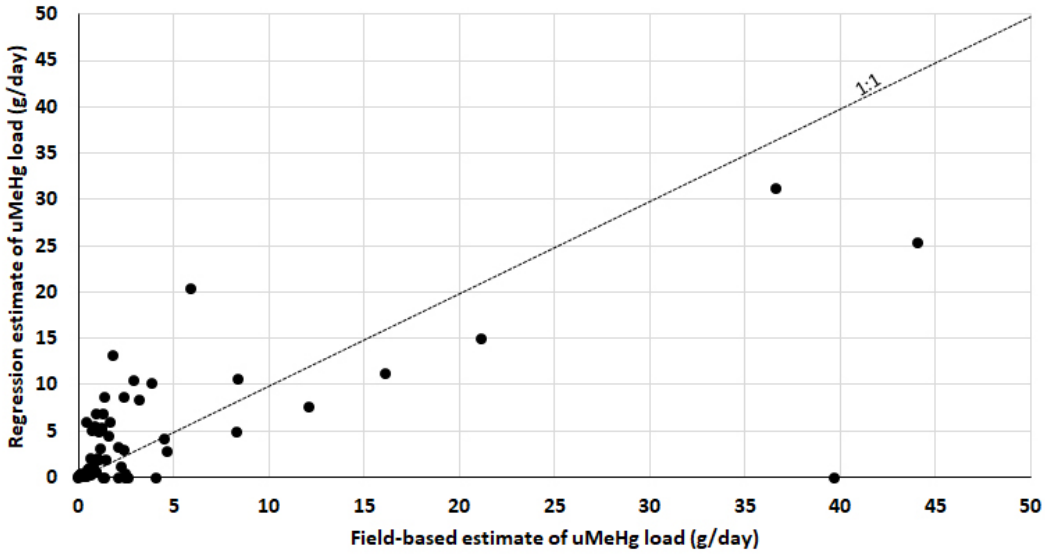

Figure Note: Data from USGS (2019)

Initial sediment bed concentrations of Hg and MeHg for each model cell (0-2 cm) were estimated using data from 2005-2016 (this study Technical Appendix F; Heim and others, 2010; Marvin-DiPasquale and others (2009). Observations from different years were combined due to limited data availability. Data were filtered to include only samples in the top 5 cm and for the months from October through May, above the stairsteps. The resulting dataset included 106 samples for Hg and 103 for MeHg. In both cases most samples (94%) were collected in 2015-2016.

Approach to Model Calibration

D-MCM was calibrated for the period from October 1996-May 2012, when necessary hydrologic information was available from the TUFLOW model (US DOI, 2019). TUFLOW hydrology used in simulations was not changed during the model calibration. It is often desirable to calibrate a model to one dataset and validate the model by applying it to a different dataset and comparing model results to observations. Due to the limited amount of available data, all observations were used to calibrate the model. It is also preferable to use data collected within the calibration period when comparing model results to observations. For this study, most of the available sediment Hg and MeHg data were collected in 2015-2016, outside the calibration period for water years 1999-2012.

Flows through Yolo Bypass are primarily unidirectional until the area known as the Stairsteps. Downstream of the Stairsteps in Liberty Island, tidal influences and two-way flows become more important. Given the limitations of TUFLOW model, and limited data for Hg, MeHg and SSC downstream of Liberty Island that become more important when there is tidal back flow, the model calibration focused on data upstream of the Stairsteps.

D-MCM results for suspended sediments and Hg were compared to field observations in the Yolo Bypass, upstream of the Stairsteps (Figure 4-1). Various model inputs ("parameters") were adjusted to improve the fit between the model and observations. This was done in two stages. First an initial manual calibration was performed, visually comparing model results to observations. This was done for suspended sediment concentrations, then Hg and finally MeHg in water and surface sediments. The manual calibration was carried out until results were subjectively deemed adequate to be used as a starting point for the final calibration using parameter estimation software (PEST ++) (See Technical Appendix H). PEST++ continued to systematically adjust selected model parameters (e.g. rate constants) to reduce the overall error between model results and observations for SSC, Hg and MeHg in water (filtered and unfiltered), and sediments (solids and porewater). Parameter estimation techniques have generally been applied previously to hydrologic models but are less commonly applied to geochemical contaminant models. Unlike the manual calibration, PEST ++ varied parameters related to suspended sediments, Hg and MeHg simultaneously in order to reduce the overall error for these three components combined. Because the number of observations available and some observation values can have order-of-magnitude differences, variable weighting was applied to allow PEST ++ to obtain a more balanced match across the different types of observations. PEST ++ software continued to adjust parameter values the best fit was obtained.

Uncertainty Analysis

The quantitative framework of the PEST++ simulations provided information used for assessing model uncertainty. For example, certainty associated with the value of the Hg(II) partitioning constant improved dramatically during the PEST analysis, while information contained in the observations provided was not

sufficient to improve certainty for the model input related to resuspension of coarse inorganic sediments (Figure 4-10). The improvement in certainty depends in part on the number and type of observations available for parameters. A related concept is identifiability (Doherty and Hunt 2009). Parameter identifiability extends traditional parameter sensitivity by accounting for confounding parameter correlation, as the both parameter sensitivity and correlation drive the performance of parameter estimation. A parameter that has higher identifiability is more constrained by information contained in the observations therefore has less room to vary. Model forecasts that depend on that parameter are therefore more certain. A parameter having low identifiability, on the other hand, is not highly constrained by observations. Parameters with low identifiability and a large influence on model results are candidates to focus future data collection \ to improve certainty associated with model results. That analysis is possible but was outside the scope of the current work.

Figure 4-10 Uncertainty Associated with Two Model Input Parameters, Prior to and Following PEST++ Analysis

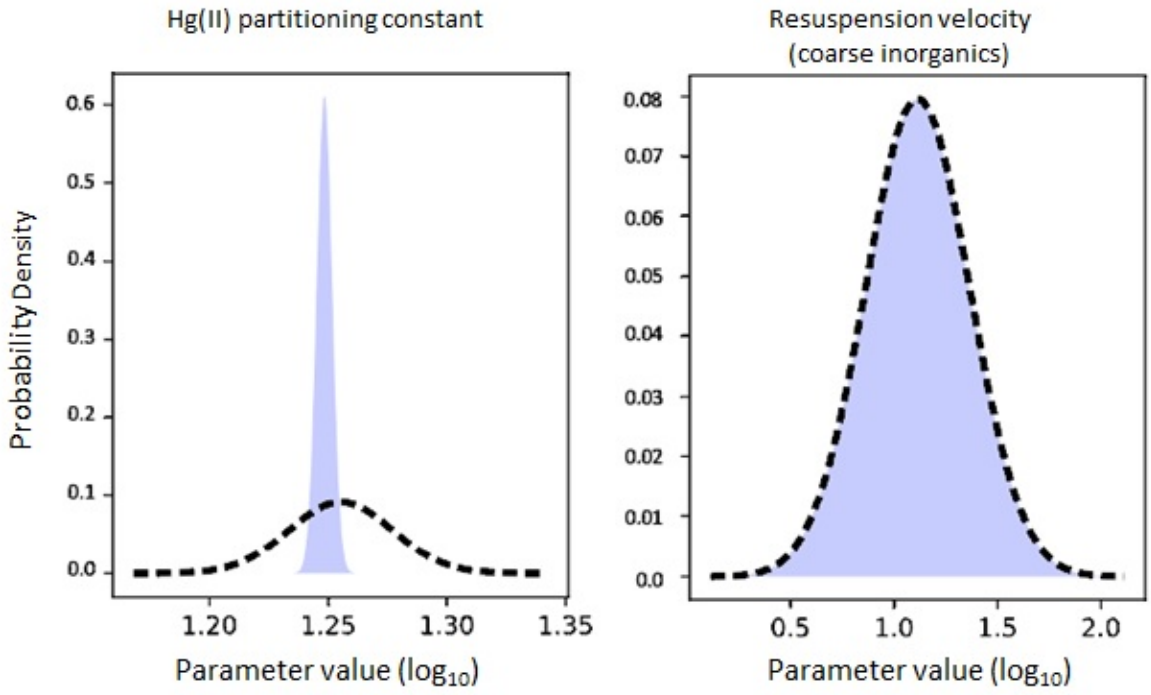

Figure Note: Dashed line = prior to PEST++ analysis. Blue area = after PEST++ analysis.

PEST++ also generated information that helped to estimate the uncertainty associated with model results. Uncertainties for two model forecasts, average annual loads averaged (1998-2012) for uHg and uMeHg, are shown in Figure 4-11. Both forecasted annual export fluxes (uHg and uMeHg) are appreciably more certain after the PEST++ calibration. An important limitation should be noted. The reported uncertainty only includes adjustable parameters included in the uncertainty analysis; all other model design and related inputs relating to process, structure and parameters are assumed to be perfectly known for the purposes of the uncertainty calculation (Hunt 2017). For example, the model assumed the pool of Hg(II) available for methylation was the dissolved concentration in sediment porewater, and that carbon turnover reflected the

activity of methylating microbes. This results in relatively smaller uncertainty ranges and should be taken as a reflection of the true uncertainty. In reality, there is significant uncertainty regarding both of these issues. In the absence of providing PEST with information to quantify these uncertainties in the conceptual model, it was effectively assuming the model approach was correct. Overall then PEST was given information allowing it to capture some but not all of the uncertainty involved in model forecasts. A second limitation is that the computationally efficient linear approach used can result in reported forecast uncertainties spanning unrealistic ranges. e.g. negative uHg export forecast in Figure 4-11 (shown in grey) prior to the PEST refinement of the calibration. More computationally intensive uncertainty approaches, such as Monte Carlo, do not exhibit this type of confounding artifact, but were not implemented in this work. Regardless, the uncertainty analysis performed conveys the primary findings regarding which model forecasts had relatively higher uncertainty, and which were most improved during calibration.

Figure 4-11 Forecasted Average Annual Export of (a) uHg and (b) uMeHg at the Stairsteps for October 1997 – May 2012

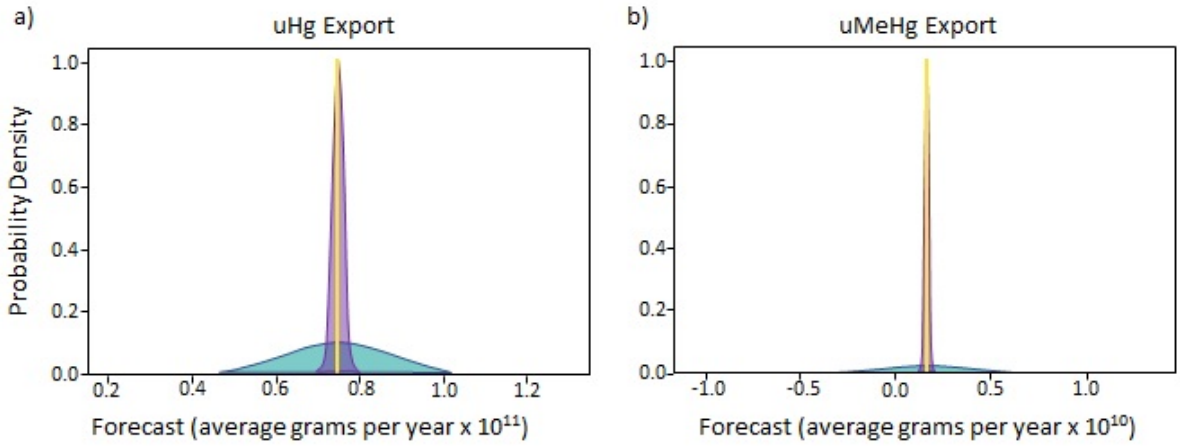

The gray bell curve is the forecast uncertainty prior to the PEST++ model calibration; the blue bell curve is the uncertainty after the PEST++ calibration. The red line is the forecasted value from the calibrated DMCM model. Note that prior uncertainty spanning a negative load forecast in (b) is a result of the approach used and does not reflect the actual probability of physically unrealistic negative loads.

Sensitivity Simulations

Following the calibration of the model to existing conditions, a series of simulations was carried out to examine the sensitivity of the model forecasts to changes in selected model inputs (Table 4-3). These simulations were developed in consultation with the Regional Board. 50% reductions were applied to the model inputs shown in Table 4-4. Simulations were carried out for the same period as the model calibration (October 1996-May 2012). The export of MeHg at the stairsteps was used as the key metric to assess the effect of each simulation.

Table 4-3 Sensitivity Analyses Agreed upon with Regional Board

Category	Goal
Particle Related	Investigate sensitivity of simulated MeHg to changes in suspended sediment inputs to the Yolo Bypass. Begin by varying suspended sediment concentrations from the Cache Creek Settling Basin (CCSB).
External Inorganic Hg Loads	Investigate sensitivity of simulated MeHg to changes in inorganic Hg inputs from tributaries to the Yolo Bypass. Begin by varying CCSB inorganic Hg concentrations to the Yolo Bypass. Investigate sensitivity of simulated MeHg to changes in atmospheric inputs.
External MeHg Loads	Investigate sensitivity of simulated MeHg to changes in MeHg inputs from tributaries to the Yolo Bypass. Begin by varying CCSB MeHg concentrations to the Yolo Bypass.
Internal MeHg Loads	Investigate sensitivity of simulated MeHg to the rate of MeHg supply generated within the Yolo Bypass.
Influence of Vegetation	Investigate sensitivity of simulated MeHg to vegetation effects in the Yolo Bypass. Begin by reducing pasture or seasonal wet-land vegetated areas in the model.

Table 4-4 Model Inputs Changed for Sensitivity Simulations

Category	Model Input Changed (50% reduction in all cases)	
Particle related	1	Cache Creek Settling Basin outflow suspended sediment concentrations
	2	Fremont Weir suspended sediment concentrations
External inorganic Hg loads	3	Cache Creek Settling Basin outflow Hg(II) concentrations
	4	Fremont Weir Hg(II) concentrations
	5	Atmospheric wet Hg(II) deposition
External MeHg loads	6	Cache Creek Settling Basin outflow MeHg concentrations
	7	Fremont Weir MeHg concentrations
Internal MeHg loads	8	Methylation rate constants in all Yolo Bypass sediments
Vegetation	9	Vegetation biomass loads to Yolo Bypass sediments

Yolo Bypass D-MCM Calibration Results

Calibration Improvement with PEST++

During the calibration of the model to existing conditions from October 1996 - May 2012, the PEST++ analysis reduced the error between observations and model estimates by 51% relative to the initial manual calibration. (Technical Appendix H)

Hydrology Results

The largest source of water to the Yolo Bypass in simulations was Fremont Weir, representing 71% of inputs for the overall period from October 1996-May 2012 (Figure 4-12a). The total amount of flow and the relative contributions of different water sources varied widely among the simulated years (Figure 4-13a, Figure 4-14a). The relative importance of Fremont Weir as a source of water varied appreciably among years, from 0-86% and was greater in wet years (expected for a flood control structure). While Knights Landing Ridge Cut represented 10% of the tributary supply of water for the overall simulation period (Figure 4-12a), it represented up to 80% of tributary inputs in dry conditions (Figure 4-14a).

Suspended Sediment Calibration Results

The greatest source of suspended sediments to the Yolo Bypass in simulations was also the Fremont Weir, representing two thirds of freshwater input for the overall period from October 1996-May 2012 (Figure 4-12b). Similar to water loads to the Yolo Bypass, the annual sediment loads and the relative contributions of different tributaries varied widely among the simulated years (Figure 4-13b, Figure 4-14b). In wet years, Fremont Weir was the largest source of suspended sediments, followed by Cache Creek Settling Basin. Knights Landing Ridge Cut was a secondary overall source of suspended sediments for the simulation period (9%), but increased in importance in dry years, representing up to 90% of tributary sediment inputs (Figure 4-14b)

Within the simulation period, suspended sediment data were available in 5 model cells upstream of the stairsteps. An example of simulated and observed suspended sediment concentrations is shown in Figure 4-15 for cell 42, a section of the Toe Drain passing the Stairsteps (Figure 4-4). Additional plots for other sites with observations are provided in Technical Appendix G.

Overall, the Yolo Bypass (to the Stairsteps) was simulated to be a net sink for suspended sediments, with less sediment exported at the stairsteps each year than loaded externally from tributaries (Figure 4-16). Overall, between October 1996 through May 2012, the loads of suspended sediments exiting the Yolo Bypass at the Stairsteps were 30% less than the sediment load entering the Yolo Bypass from its tributaries. (18-69% range among years). Trapping efficiency tended to be greater in dry years.

Figure 4-12 Average Estimated Tributary Loads of Suspended Sediment, uHg(II) and uMeHg to the Yolo Bypass, October 1996- May 2012

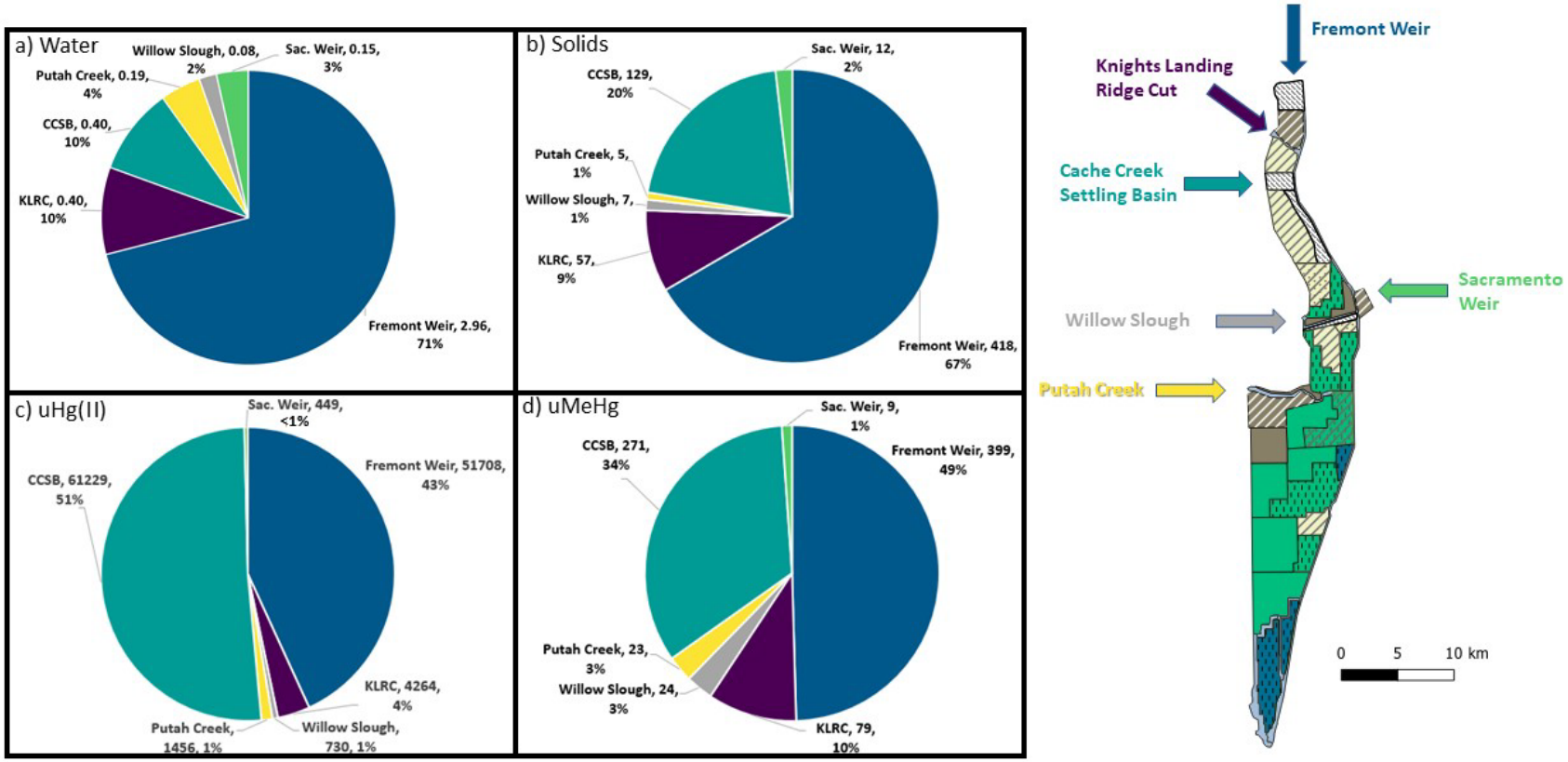

Figure Note: CCSB = Cache Creek Settling Basin, KLRC = Knights Landing Ridge Cut. Values in labels are loads and percentage of totals. Water load = km3/yr; Suspended sediment load = 1000's of tonnes/year; Hg and MeHg loads = g/yr

Figure 4-13 Estimated Tributary Loads of a) Water, b) Suspended Sediment, c) uHg(II) and d) uMeHg to the Yolo Bypass by Water Year

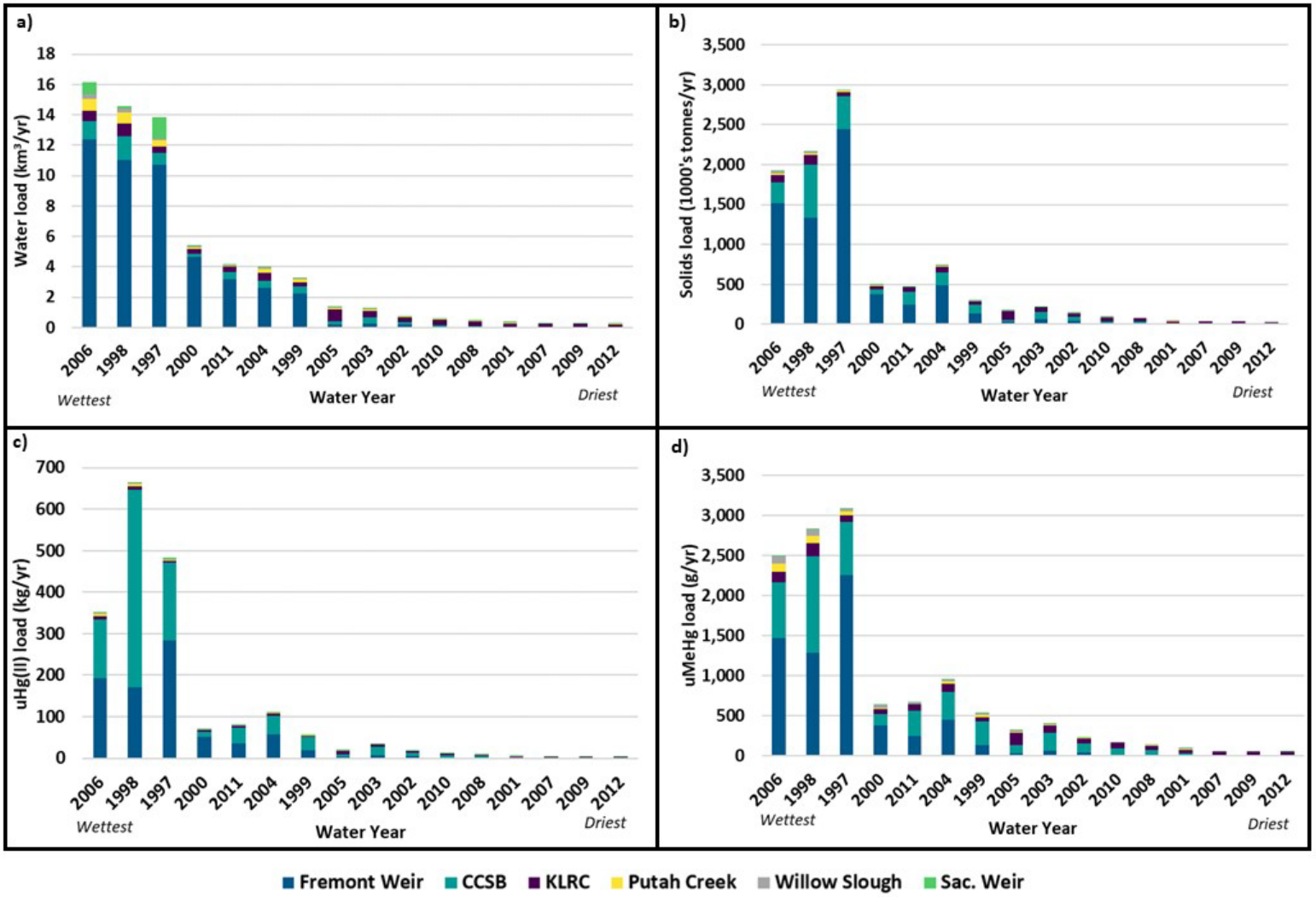

Figure Note: CCSB = Cache Creek Settling Basin, KLRC = Knights Landing Ridge Cut. Years are arranged from wettest (left) to driest (right)

Figure 4-14 Estimated Fractions of Tributary Loads of a) water, b) suspended sediment, c) uHg(II), and d) MeHg to the Yolo Bypass by water year

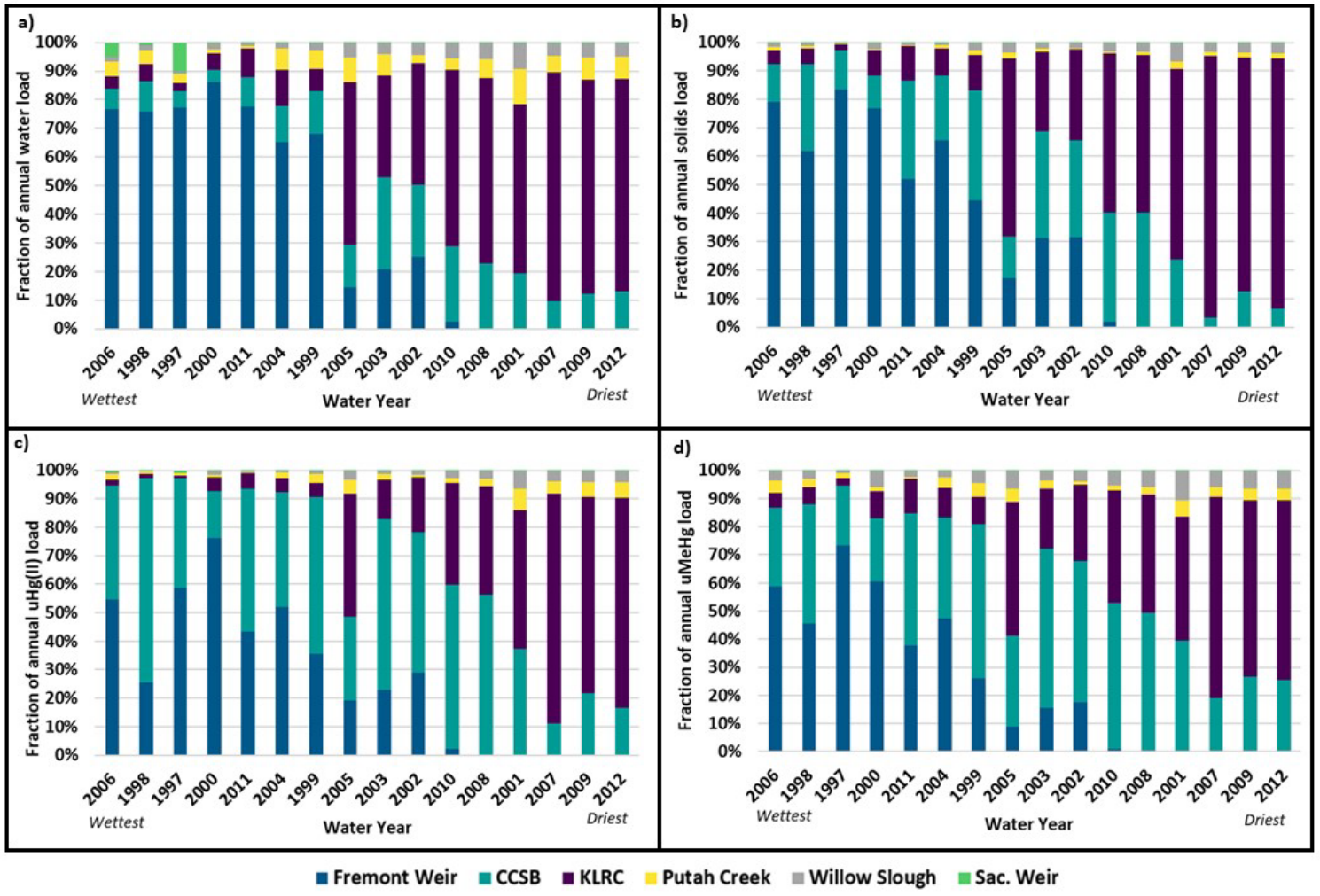

Figure Note: CCSB = Cache Creek Settling Basin, KLRC = Knights Landing Ridge Cut. Years are arranged from wettest (left) to driest (right)

Figure 4-15 Simulated and Observed Suspended Sediment Concentrations in Model Cell 42

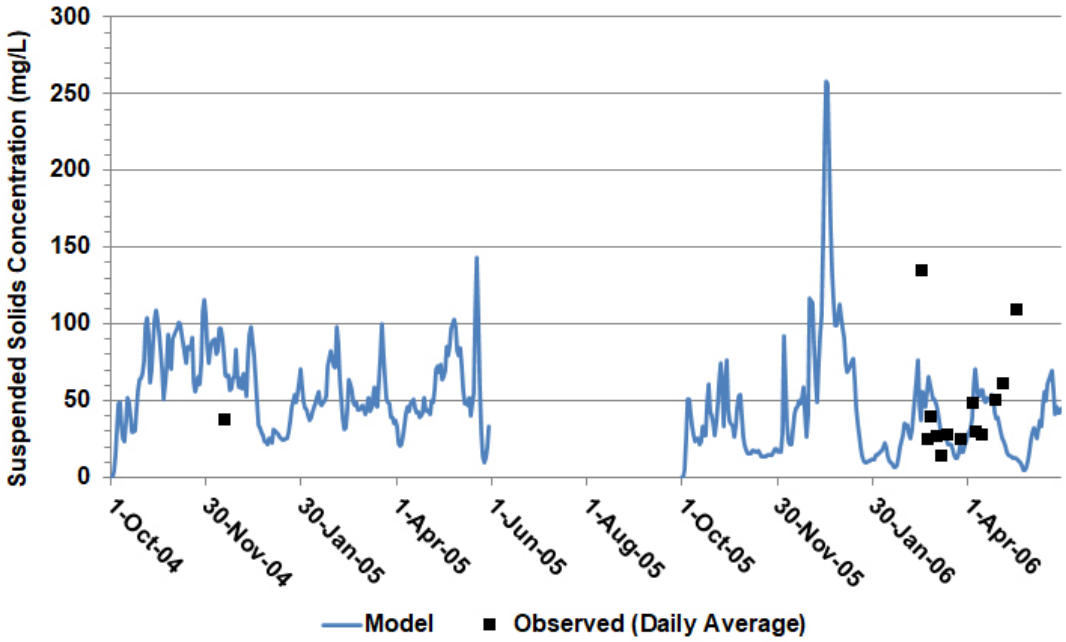

Figure Note: Cell 42 located in Toe Drain. See Figure 4-4 for location. Data from Louie and others (2008)

Figure 4-16 Simulated Yearly Ratios of Freshwater Export/Inflows for Suspended Sediments, Inorganic Hg and MeHg in the Yolo Bypass for Water Years 1997-2012

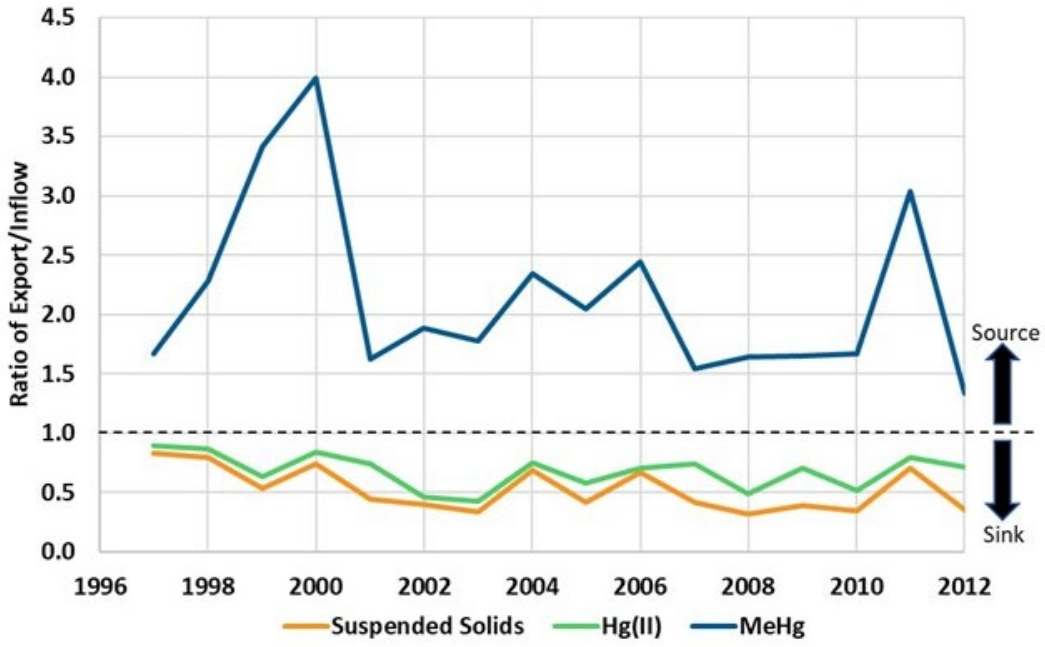

Figure Note : Values >1 = net source, Values < 1 = net sink.

Inorganic Hg Calibration

The largest estimated sources of inorganic Hg were from the Cache Creek Settling Basin and the Fremont Weir (Figure 4-12c), representing a combined 94% of the total tributary load for October 1996-May 2012. Among individual water years, Fremont Weir represented 0-76% of overall loading of inorganic Hg, while Cache Creek Settling Basin represented 11-72% (Figure 4-14d). These two sources had greater relative importance in wet years. In drier years, Knights Landing Ridge Cut was the largest estimated tributary source of inorganic Hg, up to ~80% of the annual total. Direct atmospheric loading of inorganic Hg was small, less than 3 percent of tributary loads for the simulation period. For the overall simulation period, the Yolo Bypass was a net trap for inorganic Hg (Figure 4-16), with 20 percent less exported at the stairsteps than was loaded from tributaries, (11-58% range among years). Trapping efficiency was generally greater in drier years.

For the simulation period, water column concentrations of uHg, upstream of the stairsteps, were available within the boundaries of 6 model cells upstream of the stairstep. An example of simulated and observed concentrations of uHg is shown in Figure 4-17 for a location in the Toe Drain (model cell 42). Additional plots for other sites with observations are provided in Technical Appendix G. Model simulations also reasonably reflected Hg concentrations in the surface of the sediment bed in the Yolo Bypass (Figure 4-18a), although porewater concentrations of inorganic Hg(II) were underestimated (Figure 4-18b).

Figure 4-17 Simulated and Observed Concentrations of uHg(II) in Model Cell 42

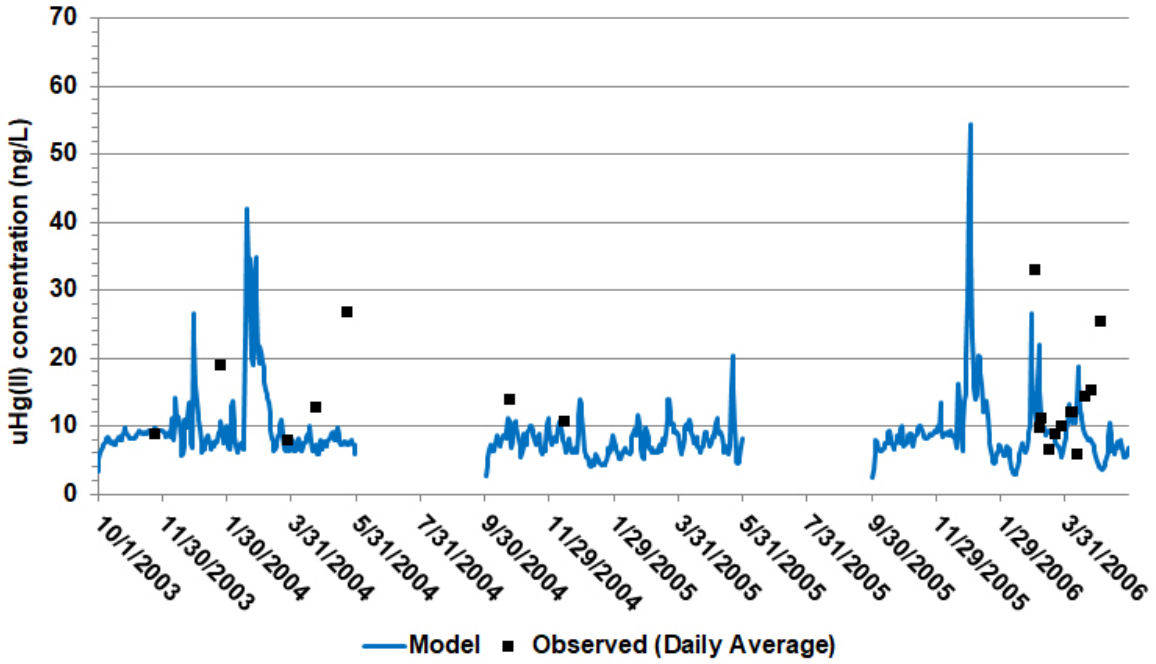

Figure Note: See Figure 4-4 for location. Data from Louie and others (2008), Larry Walker Associates (2005)

Figure 4-18 Simulated and Observed Concentrations of Hg and MeHg Surface Sediments, and Hg(II) and MeHg in Pore Waters in Yolo Bypass Model Cells

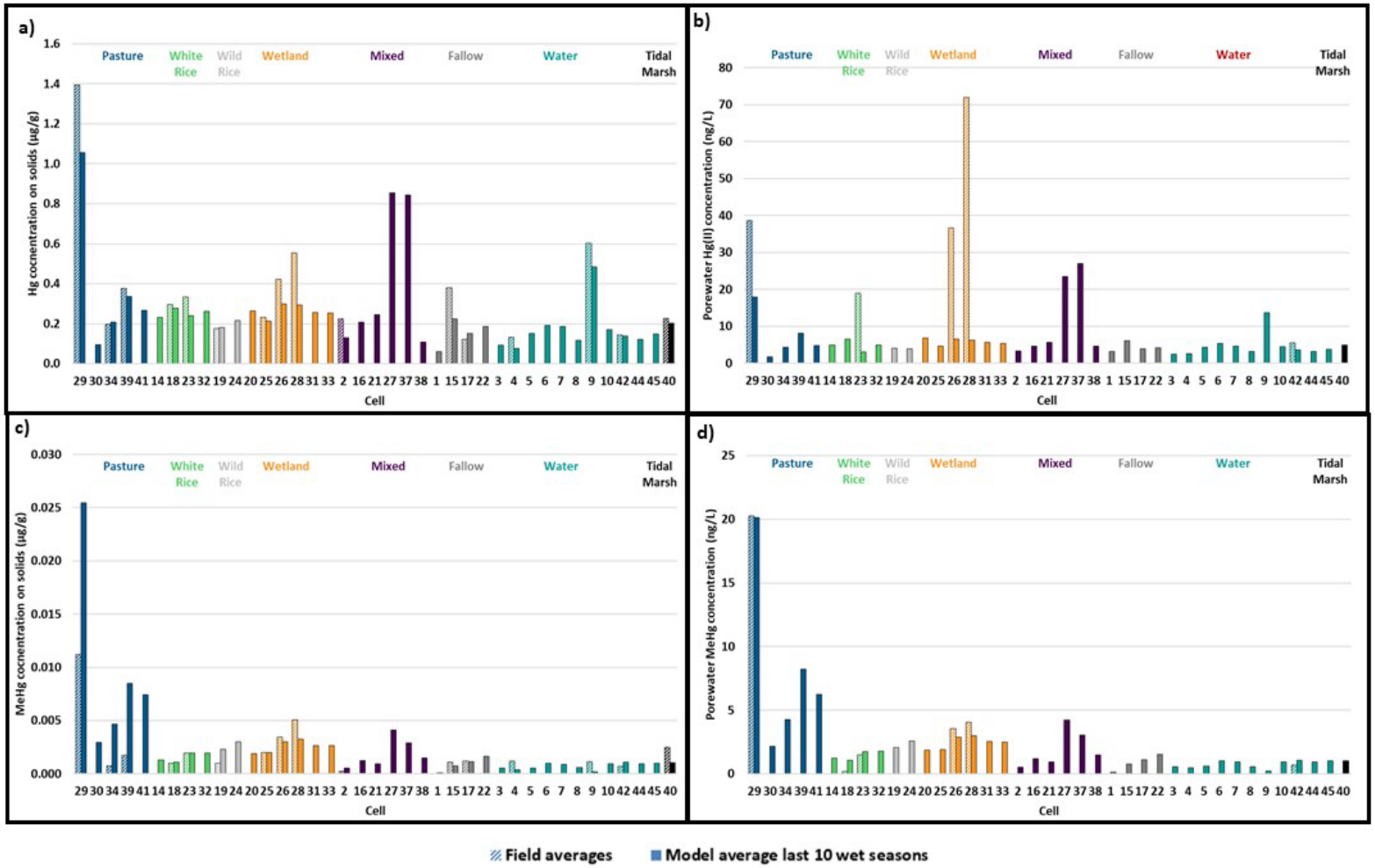

Figure Note: Model Values are averages for the last 10 wet seasons (Oct-May) of the simulation in the 2 cm thick surface layer. Observations are based on 2005-2016 (Oct-May only) data from DWR and Marvin-DiPasquale and others (2009). Cells are grouped by land use, indicated with colors. No observations were available for cells with no bars for field data.

MeHg Calibration Results

Overall, the Yolo Bypass (to the stairsteps) was simulated to be a net source for uMeHg, i.e. the export of MeHg exceeded tributary inputs. This occurred in simulations via sediment production and the associated flux to overlying waters. The average annual net load of MeHg as water passed through the Yolo Bypass (to the stairsteps) was roughly 1000 g/yr (Figure 4-19). The Yolo Bypass was a net source of uMeHg in every year simulated (export/tributary load >1.0 in all years (Figure 4-16). Atmospheric MeHg sources were small, less than 1% of the total supply. The largest tributary source of uMeHg for the overall simulation period was Fremont Weir (49% of the tributary supply) followed by Cache Creek Settling Basin (34%) (Figure 4-12d), representing a combined 83% of the total tributary uMeHg load for October 1996 - May 2012. Among individual water years, Fremont Weir represented 0-71% of tributary MeHg loading, while Cache Creek Settling Basin represented 19-57% (Figure 4-14d). Similar to tributary loading for sediments and inorganic Hg, the Fremont Weir and the Cache Creek Settling Basin had greater relative importance in wet years, while the Knights Landing Ridge Cut was more important in dry years, providing up to ~70% of the annual total MeHg supply from tributaries.

Figure 4-19 Estimated Tributary and In-Situ uMeHg Loads to the Yolo Bypass

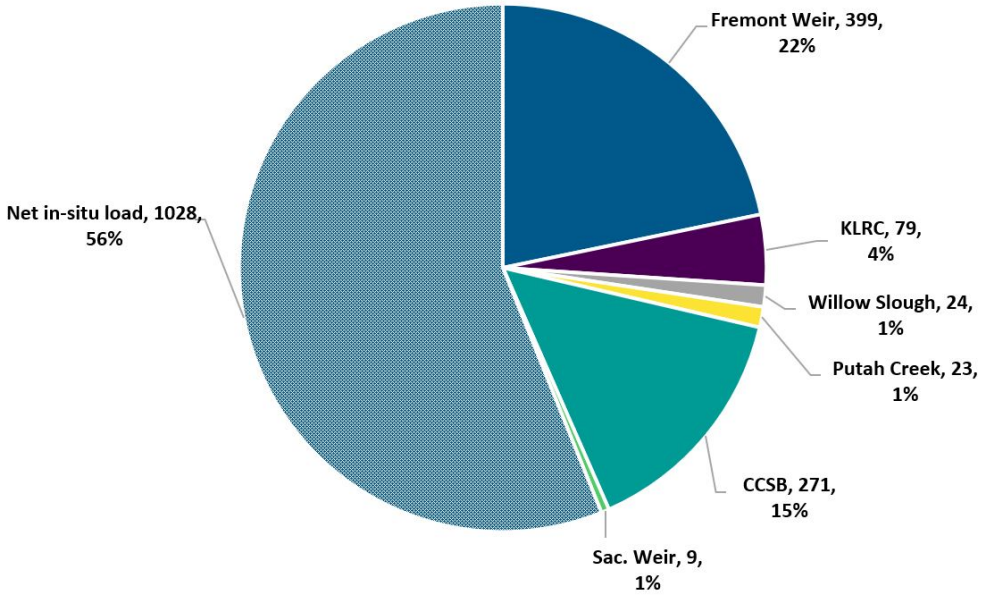

Figure Note: Values in labels are MeHg loads expressed as g/yr averages for October 1996-May 2012, and percentage of totals. KLRC = Knights Landing Ridge Cut, CCSB = Cache Creek Settling Basin, Sac. Weir = Sacramento Weir. Net in-situ load = outflows at the stairsteps minus tributary inflows.

Water column concentrations of uMeHg were available within the boundaries of 7 model cells upstream of the stairsteps for the simulation period. An example of simulated and observed concentrations of uHg is shown in Figure 4-20 for a cell in the Toe Drain (cell 42). Additional plots for other sites with observations of MeHg concentrations in water are provided in Technical Appendix G. Model simulations also reasonably reflected MeHg concentrations in surface sediments and porewater in the Yolo Bypass (Figure 4-18c and d).

Figure 4-20 Simulated and Observed uMeHg Concentrations in Model Cell 42

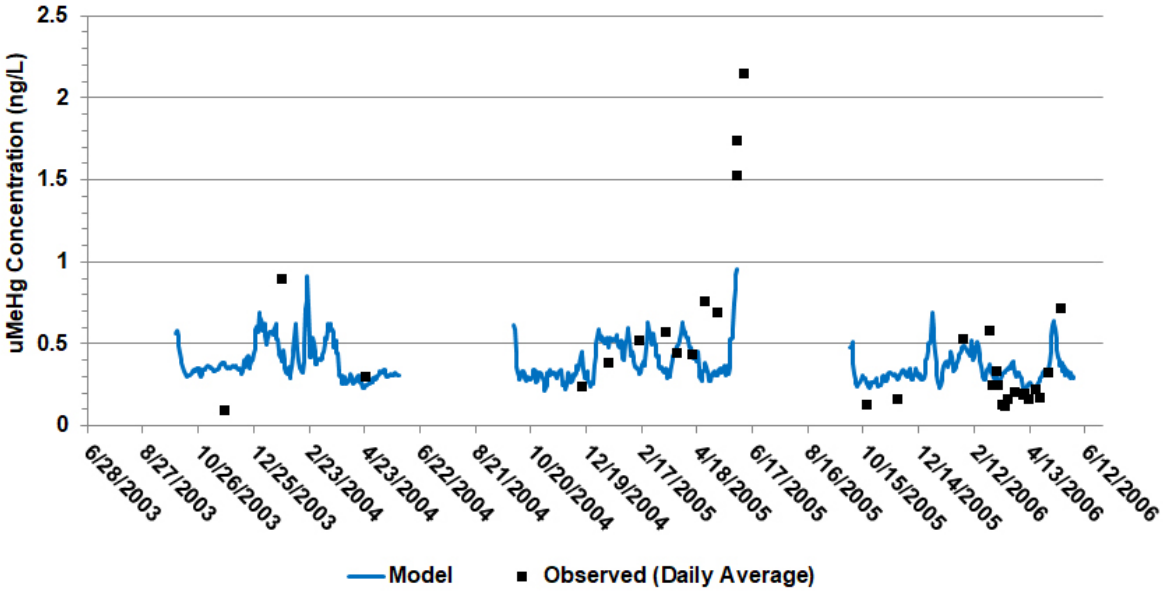

Figure Note: See Figure 4-4 for location. Data from Foe and others (2008) and Larry Walker Associates (2005).

Comparisons to Previous Studies

As a check on the performance of the model, calibration results were compared to other studies where possible. Given that different studies have different purposes and usually involve different time periods and methods, it was not expected that results would be directly comparable or identical. The purpose of the comparison was to compare in terms of general magnitudes and trends (e.g. relative importance). Examples are provided below for suspended sediment inflows and outflows (Figure 4-21), uHg tributary loads (Figure 4-22) and uMeHg tributary loads (Figure 4-23).

Figure 4-21 Comparison of Estimated Tributary Suspended Sediment Loads and Export for the Yolo Bypass, from Springborn and others (2011) and this study

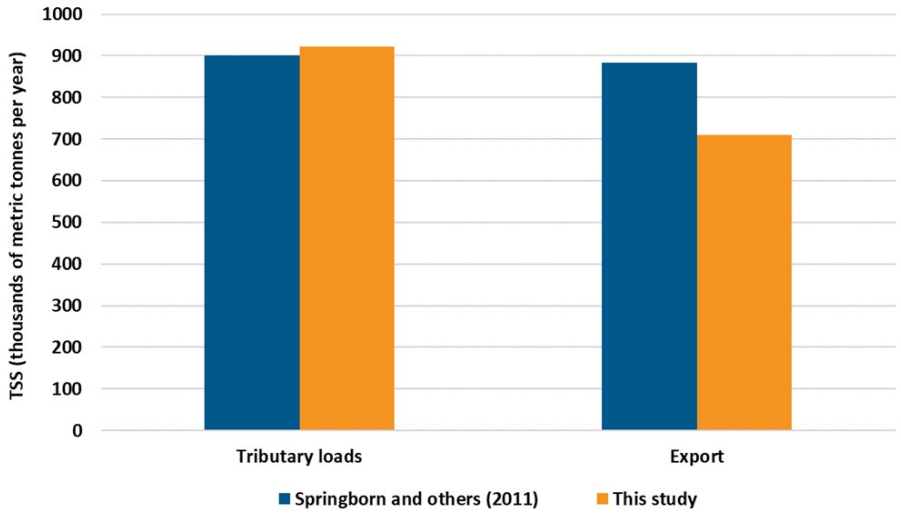

Figure Note: Tributary loads represent the sum of the Fremont Weir, the Sacramento Weir, Knight's Landing Ridge Cut, Cache Creek Settling Basin (low flow channel and overflow weir), Willow Slough, and Putah Creek. Export for this study was at stairsteps.

Figure 4-22 Comparison of Estimated Tributary uHg loads to the Yolo Bypass (1997-2003) from Springborn and others (2011) and this study

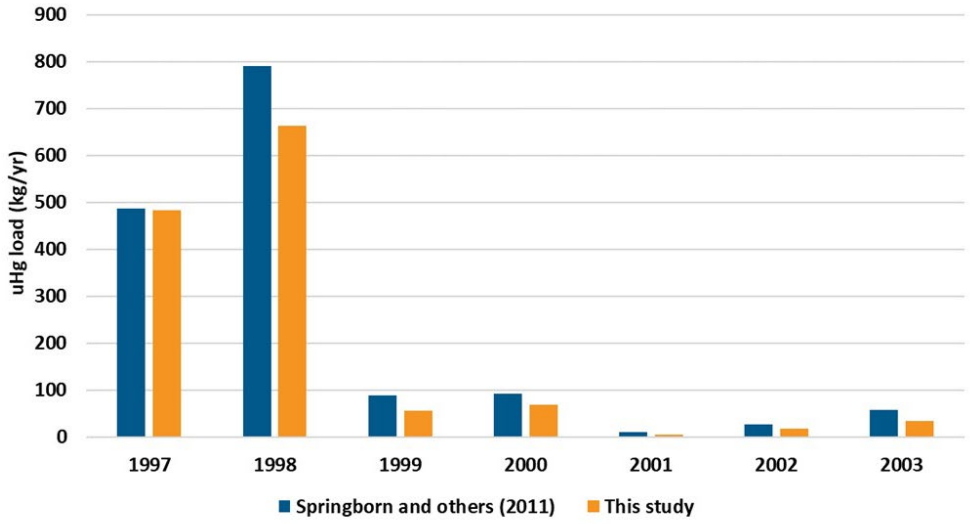

Figure Note: Tributary loads represent the sum of the Fremont Weir, the Sacramento Weir, Knight's Landing Ridge Cut, Cache Creek Settling Basin (low flow channel and overflow weir), Willow Slough, and Putah Creek.

Figure 4-23 Comparison of Estimated Tributary MeHg Loads to the Yolo Bypass for Water Years 2000-2003, from Wood and others (2011) and this study

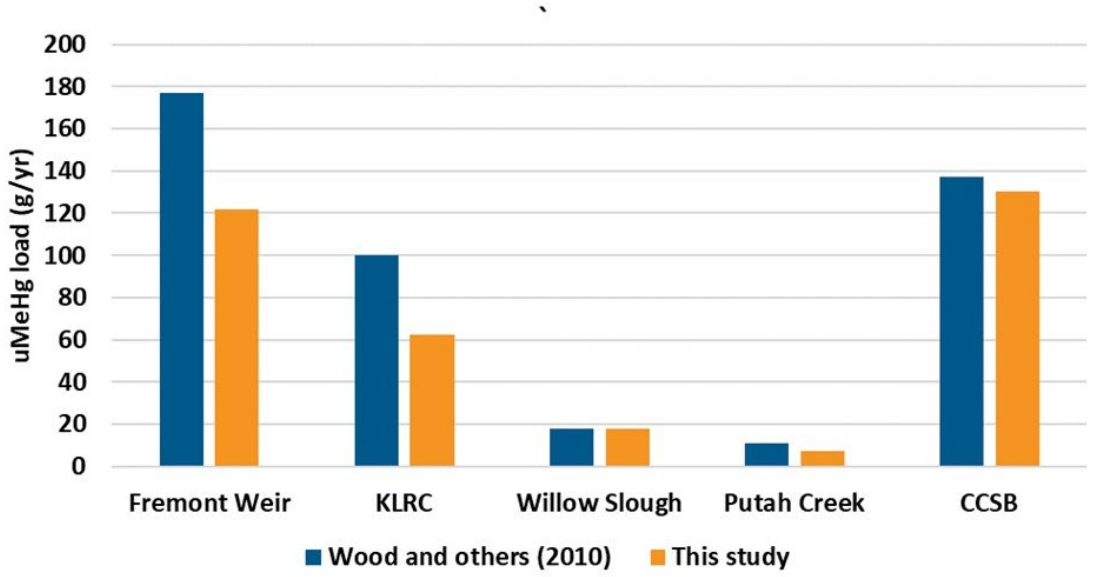

Sensitivity Scenario Results

Results for the nine scenario simulations developed by DWR and Regional Board staff (Table 4-4) are summarized in Table 4-5, in terms of the effect on the downstream export of MeHg at the stairsteps, averaged for water years 1998-2012. In some cases, the results were unexpected, and it became apparent that interpreting the simulations simply based on the modeled percent change in uMeHg export could be misleading. Overall, the simulations reduced the predicted export of uMeHg at the stairstep from less than 5% up to roughly 20%. The largest benefit was associated with the simulation reducing the efficiency of converting Hg(II) in Yolo Bypass sediments into MeHg by 50% (Simulation #8). This simulation reduced the gross production of MeHg in Yolo Bypass sediments by ~50%. The average annual net flux of MeHg from sediments to water declined by about 1/3 for water years 1998-2012. Given that the portion of the overall MeHg supply to the Yolo Bypass from tributaries was unaltered during this simulation, MeHg export at the stairsteps declined less for this simulation, roughly 20%, than the MeHg load from sediments to water.

Simulations #6 and #7, which reduced uMeHg concentrations in inflows from the CCSB and the Fremont Weir respectively, reduced MeHg export by 5-10%. Results from some of these simulations had less effect than anticipated. For example, reducing the load of suspended sediments from the CCSB (and associated Hg(II) and MeHg) had a small effect on MeHg concentrations and export in the Yolo Bypass, despite CCSB being an important source of Hg(II) in the Yolo Bypass budget. A closer examination of the simulation indicated that the 16-year simulation may not have allowed sufficient time for the effects of this simulation to be fully realized.

A simulation (#9) that reduced the supply of vegetation solids to the sediment bed after die-off by 50% produced less than a 5% decline in MeHg export. This was surprising given the results of a complementary simulation that removed all vegetation from, leading to a predicted decline of roughly 60% in net MeHg production in Yolo Bypass sediments (Figure 4-24).

Table 4-5 Summary of Simulated Effects of Sensitivity Analyses for MeHg Export from the Yolo Bypass at Stairsteps.

Category	Change to Model Inputs	Change in MeHg Export	Interpretation
Particle related	1 Reduce CCSB TSS concentrations 50%	Very small decline (<5%) ↓	The modeled decline in MeHg export from the Yolo Bypass was less than expected. This may have been related to the time required for effects to be fully evident, which may have been longer than the 16-year simulation. The decline in sediment loading slowed sedimentation rates which affected how quickly Yolo Bypass sediments responded to changes in Hg loading. It is expected that a greater decline would have occurred if the simulation could be extended for a longer simulation period.
	2 Reduce Fremont Weir TSS concentrations 50%	Minimal change ↔	Hg concentrations entering the Yolo Bypass via the Fremont Weir were lower than the average for all tributaries in simulations. Fremont Weir suspended sediments tended to "dilute" the average Hg concentrations of sediments entering the Bypass from all tributaries. Less supply of sediments over Fremont weir therefore had competing influences: (1) reduced load of Hg associated with particles, versus (2) less "dilution" of other particles entering the Bypass from other tributaries with higher Hg concentrations. The net result in the simulation was almost no change in sediment Hg concentrations and MeHg export.
External inorganic Hg loads	3 Reduce CCSB inorganic Hg concentration 50%	Very small decline (<5%) ↓	The response was less than expected. Reasons had not been clearly identified at the time of publication of this report.
	4 Reduce Fremont Weir inorganic Hg concentrations 50%	Very small decline (<5%) ↓	The response was less than expected. Reasons had not been clearly identified at the time of publication of this report.
	5 Reduce atmospheric wet Hg(II) deposition 50%	Minimal change ↔	Atmospheric Hg deposition represented less than 3% of the overall external load of inorganic Hg.
External MeHg loads	6 Reduce CCSB MeHg concentrations 50%	Modest decline (5-10%) ↓	CCSB supplied about 15% of the overall MeHg load to the Yolo Bypass in simulations (external plus internal loads). Reducing this load by 50% had a moderate effect on MeHg export at the downstream end of the system.
	7 Reduce Fremont Weir MeHg concentrations 50%	Modest decline (5-10%) ↓	Fremont Weir supplied about 20% of the overall MeHg load to the Yolo Bypass in simulations (external plus internal loads). Reducing this load by 50% had a moderate effect on MeHg export at the downstream end of the system.
Internal MeHg loads	8 Reduce methylation rate constants in all Yolo Bypass cells 50%	Moderate decline (~20%) ↓	Yolo Bypass sediments supplied about half of the overall MeHg load in simulations (external + internal). This simulation reduced MeHg production in Bypass sediments by roughly half, reducing the overall load of MeHg to the Yolo Bypass (internal + external sources) by about 20%

Category	Change to Model Inputs	Change in MeHg Export	Interpretation
Vegetation	9 Reduce vegetation biomass load to sediments 50%	Very small ⬇ declne (<5%)	This simulation reduced the supply of organic matter to Yolo Bypass sediments. Gross methylation declined about 20%, but microbial demethylation also declined. Net methylation declined about 10%. Reduced upward flux of MeHg from sediments to water was partly offset by reduced settling of MeHg from water to sediments, because of less settling sediments. Reduced vegetation inputs could reduce MeHg loads and export from the Yolo Bypass more than suggested by this simulation. See discussion of results.

Figure 4-24 Simulated Effect of Removing all Vegetation on Simulated Net MeHg Production in the Yolo Bypass

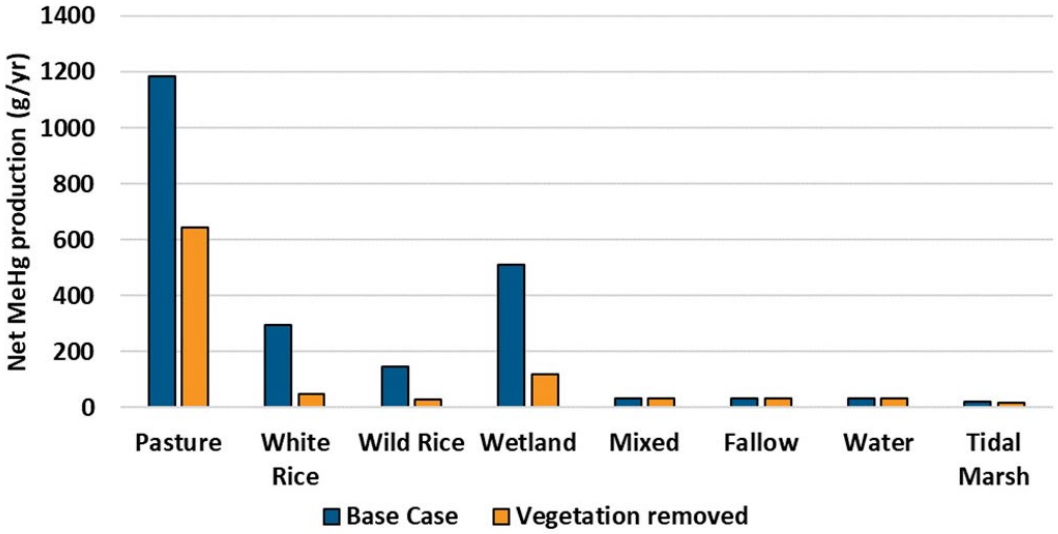

Figure Note: Net MeHg production = Sediment methylation minus sediment demethylation. Fluxes are averages above stairsteps for October 1997 – May 2012. Overall reduction in net methylation for Yolo Bypass sediments was nearly 60%. Little change occurred for net methylation in model cells without vegetation (Water channels, mixed, fallow).

Discussion

A model analysis was carried out to simulate Hg cycling in water and sediments in the Yolo Bypass, with an emphasis on sources of MeHg. It was clear prior to the model analysis that flow and sediment transport would be important processes. The model framework therefore included components for hydrology, sediment transport, inorganic Hg and MeHg in water and surface sediments. The modeling was carried out at a relatively coarse spatial resolution, representing Yolo Bypass with 47 cells (Figure 4-4). This reflected a combination of the model capabilities, data limitations and uncertainties regarding Hg cycling, such as the influence of different land use types and effects of soil wetting and drying. Increased data and knowledge of Hg cycling would be needed to warrant a higher special resolution analysis in the Yolo Bypass. Additional information is provided below.

Model Fit to Observations

Data were limited but sufficient to carry out a model calibration for suspended sediments, uHg and uMeHg for the period October 1996-2012. Data for fHg and fMeHg were included in the model calibration but were only available for 2 cells during the model calibration period (n=14 for fHg, n=9 for fMeHg) and were insufficient for calibration purposes. PEST++ significantly improved the preliminary manual calibration, reducing the overall misfit between observations and the simulation by about half. The final model calibration reasonably captured the magnitude and variability of observations in the water column (e.g.Figure 4-16, Figure 4-17, Figure 4-18). In the surface layer of the sediment bed (0-2 cm), the model also reasonable matched observed average concentrations of Hg and MeHg on solids, and pore

water MeHg concentrations (Figure 4-20). Observed pore water Hg(II) concentrations were underestimated with the model. As mentioned earlier, sediment observations were combined from 2005-2016 for Hg and MeHg due to limited data availability. This assumed no systematic change in Hg concentrations during this period. It also does not address seasonal variability that may occur for MeHg concentrations.

Simulated Hg and MeHg Fluxes

The largest estimated source of water to Yolo Bypass for the calibration period from October 1996-May 2012 was Fremont Weir (71%, Figure 4-12a). The largest external sources of suspended sediment, Hg(II) and MeHg were Fremont Weir and CCSB (Figure 4-12b,c,d). Cache Creek Settling Basin was the single largest estimated source of Hg(II) to the Yolo Bypass (51% for the overall simulation). A detailed examination the model results raised the possibility however that the Hg(II) load from the Cache Creek Settling Basin could be overestimated under high flow conditions. There were flow events during the simulation period that exceeded the flows encountered during actual field sampling programs. This meant that the regression used to estimate inorganic Hg concentrations on the basis of flow had to be applied on some occasions to conditions outside the observed range. This issue is not interpreted to put into question whether Cache Creek Settling Basin is an important source of inorganic Hg, rather it is a question of how important, and under what circumstances.

The 16-year simulation period spanned a wide range of hydrologic conditions ranging from wet to critically dry years (Table 4-2). Estimated flows from October - May ranged 65X among simulated years, based on TUFLOW modeling. In wet years, most of the freshwater load to Yolo Bypass was from Fremont Weir, while Knights Landing Ridge Cut was more important in dry years (Figure 4-13a, Figure 4-14a). Estimated tributary loads of suspended sediments, Hg(II) and MeHg also varied by more than an order of magnitude among years, strongly influenced by hydrology. Fremont Weir and the Cache Creek Settling Basin were the largest tributary sources of Hg(II) and MeHg in wet years (Figure 4-13c,d, Figure 4-14c,d). Knights Landing Ridge Cut was a secondary source of suspended sediment, Hg(II) and MeHg in wet years but became more important (in relative terms) in dry years, representing the largest individual tributary source of water, suspended sediment, Hg(II) and MeHg in some dry years.

The Yolo Bypass (to the stairsteps) was simulated to be a net trap for suspended sediments and uHg, with roughly 30% less outflow of suspended sediments, and 20% less outflow of Hg(II) at the stairsteps than loaded from tributaries. These model results are averages for the calibration period from October 1996-May 2012. For the same period, the Yolo Bypass (to the stairsteps) was simulated to be a net source for uMeHg, via sediment production and the associated flux to overlying waters. The export of MeHg at the stairsteps was roughly twice the tributary load. The net load of MeHg to water passing through the Yolo Bypass, i.e. the difference between outflow and inflow fluxes, was approximately 1000 g/yr (Figure 4-19). Most of this net load occurred during the wet season, when more of the Yolo Bypass was flooded, and flows were greater. This loading rate is comparable to net MeHg loads based on field estimates of flows and concentrations at major inflow and outflow locations in the Yolo Bypass, carried out by DWR from January 11, 2017 to April 25, 2017 (Chapter 3). The average net MeHg load from the 2017 study was 14.1 g/day (difference between outflow and inflow). The Yolo Bypass model simulations in this study did not include 2017, so direct comparisons cannot be made. However, the model average for the same date range (January 11 – April 25), for years classified as wet in Table 4-2 (2017 was a wet year), was 18 g/day (range 11-32 g/day among these wet years).

The model estimates of MeHg loading in the Yolo Bypass also compared well with the The Delta Mercury Control Program (DMCP) estimate for water years 2000-2003. Wood and others (2010) estimated a total MeHg load of 1068 g/yr to the Yolo Bypass for this period. This included 604 g/yr of loading as water passed through the Yolo Bypass, from open waters, wetlands, agricultural drainage, atmospheric deposition and NPDES facilities. The model difference between outflow and inflow fluxes for the same period was 618 g/yr. The model flux from sediments to water would be slightly greater (some of the flux from surface sediments would be photodegraded rather than exported downstream). Foe and others (2008), also estimated the Yolo Bypass to be a net source of MeHg using inflow and outflow data from water year 2006 (a wet year).

The net load of MeHg to water passing through the Yolo Bypass was influenced in simulations primarily by the net flux from sediments to overlying water, and photodegradation which removed MeHg. As a result, the flux of MeHg from sediments to water was larger than the difference between inflowing and outflowing fluxes, and is estimated to be on the order of 1200 g/yr.

Key Processes

The model analysis confirmed the key roles of hydrodynamics on Hg cycling and MeHg supply in the Delta. Increased flow led to increased tributary loads (Figure 4-13). The supply of water, suspended sediment, Hg(II) and MeHg all varied by an order of magnitude or more among the years simulated. The relative importance of tributaries also varied widely among years, depending on the hydrology, as discussed above. Flow events also led to a high degree of short term variability in simulated fluxes and concentrations of suspended sediment, Hg(II) and MeHg. The high temporal variability at different time scales, e.g. events and annual averages, has important implications when using available data to set targets for MeHg loading, and when monitoring for compliance.

The Yolo Bypass also has several other features with the potential to affect MeHg supply, including vegetation, agriculture, wetlands, excess inorganic Hg from historical mining upstream, and large tracts of land experiencing wetting and drying periods. Vegetation was an important factor affecting MeHg production in simulations. The treatment of vegetation in D-MCM is considered coarse and conceptually could be revisited. For example, after vegetation senesces in the model, vegetation solids are first delivered to the water column, where exchange can occur with surface waters. The vegetation solids then settle quickly and mix into the surface layer of the sediment bed. Effectively the vegetation supplies carbon and stimulates methylation in surface sediments. In reality, vegetation may remain sufficiently intact initially after senescence to be a distinct compartment that rests on the sediment surface where decomposition occurs. This could lead to differences in the effects of vegetation on methylation and MeHg supply to the water column, relative to the current model construct. Overall though, the model analysis suggest that vegetation has a strong influence on MeHg production in the Yolo Bypass. In simulations this effect was primarily via the additional supply of organic matter in simulations, consistent with experimental work described in Chapter 3 and studies by the US Geological Survey (e.g. Marvin-DiPasquale and others, 2014)

The D-MCM model is also constructed on the basis that higher concentrations of dissolved Hg(II) available for methylation lead to higher MeHg production. Thus areas with vegetation and higher Hg(II) concentrations in surface sediments tended to have higher MeHg concentrations (e.g. cell 29, a pasture cell in Figure 4-18). Other pasture cells with lower Hg(II) concentrations also had vegetation but lower

MeHg concentrations in surface sediments (e.g. cells 34 and 39), supporting the assumption that Hg(II) concentrations affect MeHg production, in addition to the presence of vegetation.

While wetting and drying cycles have been shown to affect MeHg production in other settings (e.g. Gilmour and others, 2004), insufficient data were available to assess this issue for the Yolo Bypass. Finally, it is important to note that large tributary sources of uHg and uMeHg do not necessarily lead to higher concentrations within the Yolo Bypass. The combination of a high flow and low concentration for a tributary could lead to a source being large relative to other tributary inputs but acting to dilute concentrations in receiving waters. If, for example, measures were taken that reduced the flow of a source with lower than the average MeHg concentration for tributaries (Fremont Weir), it might not lead to lower concentrations in Bypass waters. Additional simulations would be needed to explore this concept, but the key point is that it is important to consider concentrations as well as loads for tributaries when evaluating remedial options.

Sensitivity Scenarios

The nine sensitivity scenarios developed by DWR and Regional Board staff (Table 4-4, Table 4-5) reduced the predicted export of uMeHg at the stairsteps from less than 5% up to roughly 20%. Given that all simulations vary a specific input (e.g. tributary concentration or reaction rate constant) by 50%, the results reflect a system with multiple sources of MeHg. The simulation that reduced the gross production in Yolo Bypass sediments by half, and the net load of MeHg from surface sediments to water by 1/3, reduced MeHg export by less, about 20%, because other sources of MeHg were not changed. Regarding options to reduce the supply of MeHg from sediments to water within Yolo Bypass, the sensitivity analysis suggests that measures reducing the production of MeHg in Bypass surface sediments could be beneficial, but the challenge is identifying options that are practical in a system with a surface area exceeding 200 km^2. The model analysis, experimental studies described in Chapter 3, and previous work by the US Geological Survey collectively indicate that vegetation promotes MeHg production, at least partly by supplying labile carbon.

The net flux of MeHg from surface sediments to water included three components in the simulation: diffusion, resuspension, and settling. Diffusion and resuspension of MeHg tend to move MeHg from surface sediments to overlying water, while settling at least partially offsets the upward fluxes. Some sensitivity scenarios affected the relative balance of these three terms affecting the net load to water. For example, removing vegetation affected not just the production of MeHg, but also settling and sedimentation in simulations. Reducing tributary loads of suspended sediments reduced not just the sediment load, but also the supply of Hg(II) and MeHg, and affected sedimentation rates in the Yolo Bypass. Sedimentation rates in turn affect how quickly the surface sediment layer responds to changes in conditions, e.g. how quickly will Hg(II) and MeHg concentrations decline if loading declines? The model analysis carried out was capable of providing some initial insights into the response of the system to perturbations but in situations involving changes to the balance of multiple competing influences on MeHg supply, reliable quantification of these changes would require a better understanding and more realistic model representation of some key processes. Additional discussion is provided below.

Conclusions

An existing model of Hg cycling was combined with outputs from a hydrodynamic model and applied to Yolo Bypass waters and surface sediments. The model calibration reasonably reflected observations for

suspended sediments, Hg and MeHg concentrations in the water column and surface sediments and compared reasonably with some load estimates from other published studies. The use of parameter estimation software (PEST++) significantly improved the model fit to observations, reducing the error in the preliminary manual calibration by half. The largest external sources of sediment, Hg and MeHg for the overall 16-year simulation were Fremont Weir and CCSB, especially in wet years. KLRC was more important in dry years. Sediment production of MeHg in the Yolo Bypass and supply to overlying waters was important. The simulated export of MeHg at the stairsteps was roughly twice the inflowing tributary supply. In contrast to MeHg, less suspended and sediments and Hg(II) were exported than loaded from tributaries for the 16 year simulation period, i.e. the Yolo Bypass (to the stairsteps) was a net trap for these constituents. Vegetation and inorganic Hg concentrations both affected MeHg production in simulations. The vegetation effect was primarily via the additional supply of organic matter. Fluxes of inorganic Hg and MeHg varied by an order of magnitude or more among the years simulated, which spanned a wide range of hydrologic conditions. This has implications in terms of developing TMDL target MeHg loads and associated monitoring programs designed to determine if TMDL targets are met. A multi-year perspective is needed as well as the ability to capture short term dynamics.

Data/Knowledge Gaps and Next Steps

Data gaps: Available field data were limited in terms of characterizing boundary inflow loads, and concentrations within the Yolo Bypass, for suspended sediments, Hg and MeHg. This issue was magnified by the dynamic nature of hydrology in the Bypass, leading to a high degree of temporal and spatial variability that could not be captured with limited sampling. This constrains the current ability to quantify mercury cycling in the Yolo Bypass to a coarser perspective rather than a tightly quantified analysis. Additional data are needed to better characterize inflow loads and within-Bypass conditions for a range of hydrologic conditions and a range of years. A multi-year perspective is needed as well as the ability to capture short term dynamics. These data include measurements of inorganic Hg and MeHg in filtered, unfiltered and particulate phases in the water column and sediments, as well as ancillary data such as water chemistry and sediment characterization. Manual sampling and analysis for suspended sediments and Hg can be labor intensive and costly. Alternative options to obtain higher-frequency data should be considered, e.g. surrogates that can be sampled continuously (e.g. turbidity for suspended solids) and the use of automatic samplers for Hg.

Knowledge gaps: There are scientific gaps that also contributed to uncertainty in the model analysis, including:

- How does vegetation influence MeHg cycling and production? Better information is needed regarding the magnitude and timing of the supply of carbon and subsequent decomposition that supports MeHg production, for different land uses.
- Is the availability (for methylation) of Hg(II) contamination from legacy upstream mining similar to the availability of other sources of Hg(II)?
- Is mercury on suspended and bed sediments readily exchangeable or are some sources of inorganic Hg more important that others, in terms of supplying MeHg production? The analysis carried out in this study assumed that Hg on solids is readily exchangeable with the dissolved phase. Closely related to this question is the need for more data on filtered and particulate concentrations of inorganic Hg and MeHg in tributaries and Yolo Bypass waters.
- What is the influence of wetting and drying cycles? Wetting and drying is known to affect MeHg production. Existing data were insufficient to examine this issue in the Yolo Bypass. Field data in

surface sediments and surface waters in areas with different wetting and drying patterns would be useful, along with ancillary water chemistry (e.g. DOC, pH, redox, temperature).

Modeling Scope:

- MeHg in fish: Given that fish and shellfish MeHg levels are the ultimate end point of interest, the model analysis could be extended to include a food web and bioaccumulation component.
- Management Scenarios: Further testing of model scenarios would be beneficial. Discussions of results to-date and potential scenarios that could help identify practical solutions to reduce MeHg supply should continue.
- Climate change is altering conditions in the Delta that have the potential to affect Hg cycling and bioaccumulation (see for example, Dettinger and others, 2016 and Chapter 6). This issue should be incorporated into future assessments.
- Uncertainty: The continued used of PEST++ would be beneficial to help quantify uncertainty and identify the types of data that would most effectively reduce uncertainty in model predictions is recommended.

- **Model Development:**
  - D-MCM was an appropriate tool to use for the study reported here, given the level of data available and the state of knowledge of Hg cycling. A more realistic model analysis could be carried out using a single model that represents hydrodynamics, sediment transport, water quality and Hg cycling, capable of high spatial resolution in 2D. This is beyond the capabilities of D-MCM (or any other 2D or 3D model currently). D-MCM is not constructed in a manner amenable to such enhancements. Consider integrating Hg into an existing high-resolution model that already simulates hydrodynamics, sediment transport and water quality. This could involve using one model for the Yolo Bypass and another (DSM2-Hg) for the Delta, or a single model for the Delta and the Yolo Bypass. Preferably the software would be publicly available software.
  - The representation of vegetation in D-MCM was coarse in terms of capturing the effects of vegetation on methylation via carbon supply and decomposition. A more realistic representation of vegetation would allow better simulations of remedial options involving vegetation.
  - A supporting field program (see comments above) would be needed to take advantage of the increased model capability.

References

Atkeson, T.D., D.M. Axelrad, C.D. Pollman, and G.J. Keeler (2003) Integrating Atmospheric mercury Deposition with Aquatic Cycling in the Florida Everglades: An Approach for Conducting a Total Maximum Daily Load Analysis for an Atmospherically Derived Pollutant. Integrated Summary, Final Report.

CDEC (2020) http://cdec.water.ca.gov/reportapp/javareports?name=WSIHIST, Accessed July 20, 2020.

Department of Water Resources 2010. Fact Sheet, Sacramento River Flood Control Project Weirs and Flood Relief Structures. December 2010. Available at https://www.waterboards.ca.gov/waterrights/water_issues/programs/bay_delta/california_waterfix/exhibits/docs/STCDA%20et%20al/scda_54.pdf, Accessed: November 25, 2019.

Department of Water Resources 2015. Open Water Workgroup Progress Report. Delta Mercury Control Program. Prepared by the Open Water Workgroup and the Open Water Technical Group. Submitted to the Central Valley Regional Water Quality Control Board, Region 5, October 20, 2015. 203 pages. Avalable at: https://www.waterboards.ca.gov/centralvalley/water_issues/tmdl/central_valley_projects/delta_hg/control_studies/deltahg_oct2015pr_openwater.pdf. Accessed January 20, 2020.

Department of Water Resources (2020) Statewide Crop Mapping. Available at: https://data.cnra.ca.gov/dataset/statewide-crop-mapping). Accessed August 17, 2020.

Doherty, J., and Hunt, R.J., 2009, Two statistics for evaluating parameter identifiability and error reduction. Journal of Hydrology 366: 119-127, doi:10.1016/j.jhydrol.2008.12.018

EPRI (2013) Dynamic mercury Cycling Model for Windows 7/Vista/XP. D-MCM Version 4.0. User's Guide and Technical Reference. December 2013. Product ID 3002002518

Foe C, Louie S, and Bosworth D. (2008) Task 2. Methyl Mercury Concentrations and Loads in the Central Valley and Freshwater Delta, August 2008. In Transport, Cycling, and Fate of Mercury and Monomethyl Mercury in the San Francisco Delta and Tributaries: An Integrated Mass Balance Assessment Approach. CALFED Mercury Project Final Report, September 15, 2008.

Gilmour, C., D. Krabbenhoft, W. Orem and G. Aiken. Appendix 2B-1: Influence of Drying and Rewetting on Mercury and Sulfur Cycling in Everglades and STA Soils. Aquatic Cycling of Mercury in the Everglades (ACME) Group Preliminary Drew/Rewet Experiments (2/02 – 1/03). 2004 Everglades Consolidated Report.

Harris RC, Pollman C, Beals D, Hutchinson D. 2003a. *Modeling Mercury Cycling and Bioaccumulation in Everglades Marshes with the Everglades Mercury Cycling Model (E-MCM)*. Final Report. Prepared for the Florida Department of Environmental Protection and South Florida Water Management District. June 2003

Harris RC, Pollman C, Hutchinson D. 2003b. Wisconsin Pilot Mercury Total Maximum Daily Load (TMDL) Study: Application of the Dynamic Mercury Cycling Model (D-MCM) to Devil's Lake, Wisconsin. Submitted to the United States Environmental Protection Agency Office of Wetlands Oceans and Watersheds. December 2003

Harris RC, Rudd JWM, Amyot M, Babiarz C, Beaty KG, Blanchfield PJ, Bodaly RA, Branfireun BA, Gilmour CC, Graydon JA, Heyes A, Hintelmann H, Hurley JP, Kelly CA, Krabbenhoft DP, Lindberg SE, Mason RP, Paterson MJ, Podemski CL, Robinson A, Sandilands KA, Southworth GR, St. Louis VL, Tate MT. 2007. "Whole-ecosystem study shows rapid fish-mercury response to changes in mercury deposition." Proceedings of the National Academy of Sciences of the United States of America. Volume 104, Issue 42, Pages 16586–16591

Harris RC, Pollman C, Hutchinson D, Landing W, Axelrad D, Morey S L, Dukhovskoy D, and Vijayaraghavan K. 2012a. A Screening Model Analysis of Mercury Sources, Fate and Bioaccumulation in the Gulf of Mexico. Environmental Research, Volume 119, Pages 53-63

Harris RC, Gilmour CC, Beals C. 2012b. Effects of Climate Change on Mercury Cycling and Bioaccumulation in the Great Lakes Region. Great Lakes Atmospheric Deposition (GLAD) Program 2009 GLAD Program Contract 09-05. Prepared for the U.S. Environmental Protection Agency. October 2012

Harris RC, Hutchinson D, Beals C, Beals D, Engstrom D. 2015. Great Lakes Restoration Effects on Fish Mercury Levels. Great Lakes Restoration Initiative (GLRI). Report for Grant Agreement No. GL-00E00691-0. June 2015. Prepared for the U.S. Environmental Protection Agency

Hudson RJM, Gherini, SA, Watras CJ, Porcella, DB. 1994. Modeling the Biogeochemical Cycle of Mercury in Lakes: The Mercury Cycling Model (MCM) and Its Application to the MTL Study Lakes. In Mercury Pollution - Integration and Synthesis. C.J. Watras and J.W. Huckabee (Eds.). CRC Press Inc. Lewis Publishers

Heim, WA, Newman A, Byington A, Hughes B, Stephenson M. 2010. Spatial Distribution of Total Mercury in the Yolo Bypass: Implications for Land Use Management of Mercury Contaminated Floodplains. May 2010. Final report submitted to Chris Foe and the Central Valley Regional Water Quality Control Board.

Howitt, R., MacEwan, D., Garnache, C., Azuara, J.M., Marchand, P., Brown, D., Six, J., Lee, J. 2013. Final Report. Agricultural and Economic Impacts of Yolo Bypass Fish Habitat Proposals. Prepared for Yolo County. April 2013.

Hudson FJM, Gherini SA, Watras CJ, Porcella DB, 1994. Modeling the Biogeochemical Cycle of Mercury in Lakes; The Mercury Cycling Model (MCM) and its Application to the MTL Study Lakes. In: Watras, C.J., Huckabee, J.W. (Eds.) Mercury Pollution-Integration and Synthesis CCRC Press Inc. Lewis Publishers.

Larry Walker Associates (2005) Yolo Bypass Water Quality Management Plan Report. Prepared under CALFED Watershed Grant, Agreement # 4600001691 for the City of Woodland. May 2005

Louie, S., C. Foe, D. Bosworth (2008). Mercury and Suspended Sediment Concentrations and Loads in the Central Valley and Freshwater Delta (Task 2). Central Valley Regional Water Quality Control Board.

Marvin-DiPasquale M., C.N. Alpers, and J.A. Fleck (2009) Mercury, Methylmercury, and Other Constituents in Sediment and Water from Seasonal and Permanent Wetlands in the Cache Creek Settling Basin and Yolo Bypass, Yolo County, California, 2005−06. Open File Report 2009-1182

Marvin-DiPasquale M., L. Windham-Myers, J.L. Agee, E. Kakouros, L.H. Kieu, J.A. Fleck, C.N. Alpers, and C.A. Stricker (2014) Methylmercury production in sediment from agricultural and non-agricultural wetlands in the Yolo Bypass, California, USA. Science of the Total Environment 484: 288–299

Non-Point Source Workgroup 2012. Memo to Diane Beaulaurier, Central Valley Regional Water Quality Control Board. Subject: Knowledge Base for Nonpoint Sources Methylmercury Control Study. Available at: http://delta-mercury-nps.org/documents/NPSWorkgroup_Memo_KnowledgeBase.pdf, Accessed: July 22, 2020.

Sacramento River Forum (2020) https://www.sacramentoriver.org/forum/index.php?id=gismy&rec_id=5 accessed 7/17//2020

Schmitt M, 2011. Natural Resources Defense Council. Building River: The Yolo Bypass-Hiding in Plain Sight https://www.nrdc.org/experts/monty-schmitt/building-rivers-yolo-bypass-hiding-plain-sightAccessed 7/2/2020

Springborn M, Singer MB, Dune T. 2011. "Sediment-adsorbed total mercury flux through Yolo Bypass, the primary floodway and wetland in the Sacramento Valley, California." Science of the Total Environment, Volumes 412-413. Pages 203-213.

Stephenson, M. (2020) Spreadsheet titled MeHg mass estimates Vegsens 3-17-20.xlsx

Stephenson, M. (2019) Information forwarded in email from C. DiGiorgio to R. Harris July 19, 2019

Stephenson, M. (2017) Spreadsheet titled Stephenson (2017) biomass of plants.xlsx

Suddeth Grimm R, Lund JR. 2016. "Multi-Purpose Optimization for Reconciliation Ecology on an Engineered Floodplain: Yolo Bypass, CA." San Francisco Estuary and Watershed Science, Volume 14, Issue 1, Article 5, 23 Pages

Tsai, P. and R. Hoenicke (2001) San Francisco Estuary Regional Monitoring Program for Trace Substances. San Francisco Bay Atmospheric Deposition Pilot Study Part 1: Mercury. SFEI Contribution 72. July 2001. San Francisco Estuary Institute

TUFLOW. Viewed online at: https://www.tuflow.com. Accessed: September 10, 2019.

US DOI, Bureau of Reclamation/DWR. 2019. Yolo Bypass Salmonid Habitat Restoration and Fish Passage, Final Environmental Impact Statement/Environmental Impact Report, Appendix D. May 2019. Available at: https://www.usbr.gov/mp/nepa/nepa_project_details.php?Project_ID=30484. Accessed July 20, 2020.

U.S. Fish and Wildlife Service. 2020. National Wetlands Inventory. Available at: https://www.fws.gov/wetlands/. Accessed. July 6, 2020.

US Geological Survey (2019) Spreadsheet titled "CCSB_DWR_NWIS.AQ_wy2010-19_SSC-Hg_to-Reed-Harris_8Nov2019.xlsx" emailed from C. Alpers to R. Harris, November 9, 2019.

Wood, ML, Foe CG, Cooke J, Louie SJ. 2010. Sacramento – San Joaquin Delta Estuary TMDL for Methylmercury. Staff Report – Regional Water Quality Control Board, Central Valley Region. Rancho Cordova, California. Viewed at: https://www.waterboards.ca.gov/centralvalley/water_issues/tmdl/central_valley_projects/delta_hg/archived_delta_hg_info/april_2010_hg_tmdl_hearing/apr2010_tmdl_staffrpt_final.pdf

Wyndham-Myers, L., M. Marvin-DiPasquale, E. Kakouros, J.L. Agee, L.H. Kieu, C.A. Stricker, J.A. Fleck, and J.T. Ackerman (2014). Mercury cycling in agricultural and managed wetlands of California, USA: Seasonal influences of vegetation on mercury methylation, storage, and transport